the induction of secretory IgA (sIgA) [1]. Dimeric (or polymeric) forms of IgA antibodies, produced by plasma cells that have differentiated from IgA^+ B cells in the lamina propria region, bind to polymeric Ig receptors (pIgR) expressed by epithelial cells to form sIgA. This sIgA is then transported into the gut lumen, leading to the creation of the first line of defense offered by the humoral arm of mucosal immunity.

Evidences for the Presence of Craniofacial Mucosal Immune System

Induction and regulation of intestinal mucosal immunity have been extensively elucidated. Parts of gut-associated lymphoid tissue (GALT), such as PPs, play a central role as the inductive tissue responsible for the initiation of an antigen-specific IgA response [3]. In contrast, the respiratory mucosal immune system is less well understood due to the complexity of immunological defenses of the upper and lower respiratory tracts. In general, the upper respiratory tract has been shown to be predominantly protected by mucosal immunity, and the lower respiratory tract protected by a mixture of both mucosal and systemic immunity, respectively. NALT has been identified as a pair of bell-shaped lymphoid tissues situated at the bottom of the nasal cavity in rodents [4, 5] (fig. 1). Although NALT has not been anatomically located in the adult human nasal cavity, a previous report has indicated that NALT-like structures are found only in human infants [6]. Although tonsils are seen in humans and not rodents [7], and the anatomical location of NALT is different for rodents and humans, Waldeyer's ring (seen in humans) is believed to be an analog of murine NALT [8]. The NALT epithelium contains M cells [9]. As NALT B cells express activation-induced cytidine deaminase (AID), class switch recombination from μ to α heavy chains can be induced [10]. Thus, NALT has been shown to be the site for the generation of memory-type IgA^+ B cells. Th1/Th2-type cells and cytotoxic T cells are also induced in NALT after nasal immunization or infection [4]. These findings suggest that NALT fulfils the necessary immunological criteria as an inductive tissue for the upper respiratory tract against inhaled antigens.

In addition to NALT, we have recently reported that an organized lymphoid structure of TALT was found in the murine lacrimal sac, adjacent to the tear duct [11] (fig. 1). Although TALT has also been identified in the human tear duct which connects the ocular and nasal cavities [12], its function is still unclear. Extensive analysis of murine TALT has been done to elucidate its role in the induction and regulation of antigen-specific immune responses against ocular antigens. TALT possesses FAE, which contains M cells and is distinct from the lacrimal mucus membrane. B cells and DCs accumulate in the subepithelial dome lesion, forming lymphoid follicle like PPs and NALT. As we have shown, mice were immunized by administering eye drops containing cholera toxin (CT), both the formation of germinal centers for IgA^+ B cell responses and the induction of antigen-specific Th cells were observed in TALT [11]. Furthermore, ocular immunization resulted in the initiation of antigen-specific T and B cell responses in NALT due to the traveling of the antigen from the ocular surface to the nasal cavity via the tear duct [11]. Thus, our results suggest that TALT plays an important role for not only ocular, but also nasal immune responses, and that ocular immunization induces antigen-specific IgA response via both TALT- and NALT-mediated mucosal immune systems. Another type of lymphoid tissue believed to be involved in the induction of protective immunity for the ocular surface is the conjunctiva-associated lymphoid tissue (CALT) which develops in mammals other than rodents as a small lymphoid follicle in the conjunctiva [13]. Yet another member of the craniofacial immune system is the tubal tonsil located at the entrance of the Eustachian tube, and thought to be associated with the middle ear mucosa and hence, ear

Table 1. Unique organogenesis programs of the craniofacial mucosal immune system – comparing with PPs

	PPs	NALT	TALT
Chronological development	prenatal	postnatal	
CXCR5-CXCL13 CCR9-CCL25 (chemokine)	dependent	independent	
LTα1β2-LTβR IL7-IL7R (cytokine)	dependent	independent	
α4β1 integrin-VCAM1 (adhesion molecule)	dependent	independent	
RORγt (transcription factor)	dependent	independent	
Id2 (gene)	dependent		independent

immunity. Thus, it is natural and logical to consider the mucosal immune system regulated by these different MALTs situated in the craniofacial area, such as NALT, TALT, CALT, and Waldeyere's ring tonsils, as an organized craniofacial immune system.

Uniqueness in the Development of Craniofacial Mucosal Immune System

The major organized lymphoid structures of the craniofacial mucosal immune system, such as NALT and TALT, have been shown to possess a unique organogenesis program when compared with other secondary lymphoid tissues such as the PPs (table 1) [5, 11]. Chronological examination of tissue development revealed that genesis of most of the secondary lymphoid tissues, including PPs and peripheral lymph nodes (pLNs), was initiated during the prenatal stage [14]. In contrast, the development of NALT and TALT started only after birth [5, 11]. In addition, essential organogenesis molecules required for the development of PPs and other lymphoid tissues were all found to be dispensable for the formation of NALT [5] and TALT [11]. For example, retinoic orphan receptor RORγt, a molecule associated with the transcription machinery and found to be indispensable for the development of PPs and pLNs [14], is not required for the development of NALT and TALT [5, 11]. Similarly, neither the IL-7/IL-7R cytokine family nor the LTα1β2-LTβR signaling pathways, which are involved in the genesis of PPs and pLNs, have been found to be essential for NALT and TALT genesis. Interestingly, even Id2, another well-known transcriptional molecule for lymphoid tissue genesis that is essential for the development of PPs, pLNs, and NALT, is dispensable for TALT genesis. RORγt serves as the master regulator of gut immunity (in terms of chemokine expression) [15], and of the generation of regulatory T and Th17 cells [16]. We expect that such molecules must be involved in the regulation of the craniofacial mucosal immune system operated by NALT and TALT, but that they have not yet been identified.

Craniofacial Immune System and Vaccine Development: A New Type of Mucosal Vaccine

As many pathogens are transmitted via the mucosal surfaces of the respiratory route, it is desirable to develop an effective vaccine that can provide a first-line defense against respiratory pathogens. Vaccines administered via the mucosal route are ideal as they can induce both systemic and mucosal immune responses, resulting in the induction of two layers of protection. Nasal vaccines have been shown to be effective for the induction of viral antigen-specific

immunity for the craniofacial immune system [17, 18]. FluMist®, derived from cold-adapted influenza virus, is currently available as a nasal vaccine [19]. Our laboratory has recently reported a new nanotechnology-based, nasal vaccine antigen delivery system for a subunit vaccine [20]. Nanogel is a nanometer-sized hydrogel which can be fused with a protein antigen and act as an artificial chaperone for the delivery of the native form of the vaccine antigen to epithelial cells and APCs, such as DCs, when given via the nasal route. It should be noted that a cationic form of nanogel enhances the longevity of its adhesion to the nasal epithelium, leading to effective vaccine antigen delivery to mucosal dendritic cells in the nasal cavity for the initiation of antigen-specific immune response. Nasal cationic-nanogels containing vaccine antigens (e.g. *Clostridium botulium* toxoid and tetanus toxoid) have thus been shown to be effective in the induction of antigen-specific systemic IgG and nasal IgA responses without the co-administration of adjuvants. This vaccine antigen delivery system can avoid the transmission of the vaccine component to the central nervous system through the olfactory epithelium [21].

Our understanding of the ocular immune system, including TALT, led us to consider the development of an ocular or eye drop vaccine. Although effectively able to induce mucosal and systemic immunity, our ocular vaccine is still undergoing preclinical safety evaluation and is not yet ready for clinical use. A better understanding of the craniofacial immune system will facilitate the development of novel mucosal vaccines, which can contribute to the prevention and control of respiratory and ocular infectious diseases.

References

1 Mestecky J, Blumberg R, Kiyono H, McGhee JR: Fundamental Immunology, ed 5. San Diego, Academic Press, 2003, pp 965–1020.

2 Mora J, Iwata M, Eksteen B, Song S, Junt T, Senman B, Otipoby KL, Yokota A, Takeuchi H, Ricciardi-Castagnoli P, Rajewsky K, Adams DH, Andrian UH: Generation of gut-homing IgA-secreting B cells by intestinal dendritic cells. Science 2006;314:1157–1160.

3 Kiyono H, Fukuyama S: Nalt- versus Peyer's-patch-mediated mucosal immunity. Nat Rev Immunol 2004;4: 699–710.

4 Yanagita M, Hiroi T, Kitagaki N, Hamada S, Ito H, Shimauchi H, Murakami S, Okada H, Kiyono H: Nasopharyngeal-associated lymphoreticular tissue (NALT) immunity: fimbriae-specific Th1 and Th2 cell-regulated IgA responses for the inhibition of bacterial attachment to epithelial cells and subsequent inflammatory cytokine production. J Immunol 1999;162:3559–3565.

5 Fukuyama S, Hiroi T, Yokota Y, Rennert P, Yanagita M, Kinoshita N, Terawaki S, Shikina T, Yamamoto M, Kurono Y: Initiation of NALT organogenesis is independent of the IL-7R, LTβR, and NIK signaling pathways but requires the Id2 gene and $CD3^{-}CD4^{+}CD45^{+}$ cells. Immunity 2002;17:31–40.

6 Debertin AS, Tschernig T,Tönjes H, Kleemann WJ, Tröger HD, Pabst R: Nasal-associated lymphoid tissue (NALT): frequency and localization in young children. Clin Exp Immunol 2003;134:503–507.

7 Kuper CF, Koornstra PJ, Hameleers DM, Biewenga J, Spit BJ, Duijvestijn AM, van Breda Vriesman PJ, Sminia T: The role of nasopharyngeal lymphoid tissue. Immunol Today 1992;13:219–224.

8 Kuper C, Hameleers D, Bruijntjes J, Ven I: Lymphoid and non-lymphoid cells in nasal-associated lymphoid tissue (NALT) in the rat. Cell Tissue Res 1990;259:371–377.

9 Park H, Francis K, Yu J, Cleary PP: Membranous cells in nasal-associated lymphoid tissue: a portal of entry for the respiratory mucosal pathogen group A Streptococcus. J Immunol 2003;171:2532–2537.

10 Shimoda M, Nakamura T, Takahashi Y: Isotype-specific selection of high affinity memory B cells in nasal-associated lymphoid tissue. J Exp Med 2001;194: 1597–1607.

11 Nagatake T, Fukuyama S, Kim D-Y, Goda K, Igarashi O, Sato S, Nochi T, Sagara H, Yokota Y, Jetten AM, Kaisho T, Akira S, Mimuro H, Sasakawa C, Fukui Y, Fujihashi K, Akiyama T, Inoue J-i, Penninger JM, Kunisawa J, Kiyono H: Id2-, RORγt-, and LTβR-independent initiation of lymphoid organogenesis in ocular immunity. J Exp Med 2009;206:2351–2364.

12 Knop E, Knop N: Lacrimal drainage-associated lymphoid tissue (LDALT): a part of the human mucosal immune system. Invest Ophthalmol Vis Sci 2001;42:566–574.

13 Cain C, Phillips T: Developmental changes in conjunctiva-associated lymphoid tissue of the rabbit. Invest Ophthalmol Vis Sci 2008;49:644–649.

14 Eberl G, Marmon S, Sunshine M, Rennert P, Choi Y, Littman D: An essential function for the nuclear receptor RORγt in the generation of fetal lymphoid tissue inducer cells. Nat Immunol 2003;5:64–73.

15 Iwata M, Hirakiyama A, Eshima Y, Kagechika H, Kato C, Song SY: Retinoic acid imprints gut-homing specificity on T cells. Immunity 2004;21:527–538.
16 Zhou L, Lopes J, Chong M, Ivanov I, Min R, Victora G, Shen Y, Du J, Rubtsov Y, Rudensky A: TGF-β-induced Foxp3 inhibits Th17 cell differentiation by antagonizing roryt function. Nature 2008;453:236–240.
17 Imaoka K, Miller C, Kubota M, McChesney MB, Lohman B, Yamamoto M, Fujihashi K, Someya K, Honda M, McGhee JR, Kiyono H: nasal immunization of nonhuman primates with simian immunodeficiency virus p55gag and cholera toxin adjuvant induces Th1/Th2 help for virus-specific immune responses in reproductive tissues. J Immunol 1998;161:5952–5958.
18 Kurono Y, Yamamoto M, Fujihashi K, Kodama S, Suzuki M, Mogi G, McGhee J, Kiyono H: Nasal Immunization Induces *Haemophilus influenzae*-specific Th1 and Th2 responses with mucosal IgA and systemic IgG antibodies for protective immunity. J Infect Dis 1999;180:122–132.
19 Jackson LA, Holmes SJ, Mendelman PM, Huggins L, Cho I, Rhorer J: Safety of a trivalent live attenuated intranasal influenza vaccine, FluMist, administered in addition to parenteral trivalent inactivated influenza vaccine to seniors with chronic medical conditions. Vaccine 1999;17:1905–1909.
20 Nochi T, Yuki Y, Takahashi H, Sawada S, Mejima M, Kohda T, Harada N, Kong I, Sato A, Kataoka N, Tokuhara D, Kurokawa S, Takahashi Y, Tsukada H, Kozaki S, Akiyoshi K, Kiyono H: Nanogel antigenic protein-delivery system for adjuvant-free intranasal vaccines. Nat Mater 2010;9:572–578.
21 Mutsch M, Zhou W, Rhodes P, Bopp M, Chen R, Linder T, Spyr C, Steffen R: Use of the inactivated intranasal influenza vaccine and the risk of Bell's Palsy in Switzerland. N Engl J Med 2004;350:896–903.

Hiroshi Kiyono
Division of Mucosal Immunology, Department of Microbiology and Immunology
Institute of Medical Science, University of Tokyo
4–6–1 Shirokanedai, Minato-ku, Tokyo 108-8639 (Japan)
Tel. +81 3 5449 5271, E-Mail kiyono@ims.u-tokyo.ac.jp

Epithelial cell microRNAs in gut immunity

Yoshiyuki Goto & Hiroshi Kiyono

MicroRNAs regulate many biological functions. Research now indicates that intestinal epithelial microRNAs might also regulate the differentiation of goblet cells and promote T helper type 2 immune responses to parasite infection.

The intestine is a unique organ that is constantly exposed to an almost limitless array of foreign antigens, including not only innocuous food-derived materials and harmless commensal microbes but also pathogenic bacteria, viruses and parasites. The establishment and maintenance of appropriate immune quiescence or activity in the gut mucosa requires highly sophisticated immunological regulatory systems generated by the cooperative interaction between intestinal epithelial cells and mucosal cells of the immune response. Among numerous regulatory molecules, microRNAs (miRNAs) have received much attention as a newly identified family of regulators in animal and plant cells. Although the critical function of these small RNAs is suggested to contribute to the establishment of immunological homeostasis at mucosal sites, only limited information on this is available at present. Now a study by Biton *et al.* in this issue of *Nature Immunology* reports on how intestinal epithelial miRNAs might regulate the differentiation of goblet cells and the associated development of antiparasitic T helper type 2 (T_H2) immunity[1].

The intestine is covered by an epithelial monolayer comprising four main types of intestinal epithelial cells: columnar epithelial cells, paneth cells, endocrine cells and goblet cells[2]. These epithelial cells form the first physical barrier that separates the host from the external environment. In addition, epithelial cells also detect stimuli from luminal antigens and transmit signals to the various innate and acquired types of mucosal cells of the immune response for the initiation of active or quiescent immune responses. Epithelial cells and mucosal cells of the immune response thus tightly regulate each other, and this crosstalk results in intestinal immunological homeostasis. For example, thymic stromal lymphopoietin (TSLP) produced by epithelial cells limits the production of proinflammatory cytokines by dendritic cells[3], whereas the proliferation and differentiation of epithelial cells is controlled by epithelial cell growth factors such as keratinocyte growth factor generated from intestinal T cells[4]. Further, bilateral regulation of intestinal T_H1 cells versus T_H2 cells and of cells of the T_H17 subset versus regulatory T cells has a critical role in gut immunological homeostasis. Whereas the differentiation of T_H17 cells and regulatory T cells is regulated by commensal bacteria[5–7], the nature of the various pathogens influences the outcome of T_H1- and T_H2-mediated immunity; for example, helminths tend to drive T_H2 development[8]. Helminth-derived antigens are taken up by mucosal dendritic cells and basophils, which leads to the differentiation of T_H2 cells from naive T_H0 cells[8]. T_H2 cytokines such as interleukin 4(IL-4), IL-5 and IL-13 accelerate helminth-specific T_H2-biased immunity[8]. It should be remembered that epithelial cells occupy a physically and perhaps immunologically intermediate position between the parasites and gut mucosal immunity. Epithelial cell–derived TSLP thus promotes T_H2 immune responses by 'educating' intestinal dendritic cells during infection[3]. However, the precise cellular and molecular mechanisms by which epithelial cells establish gut T_H2 immunity are still not fully understood.

The maturation of miRNA occurs via a series of steps. Two main RNase III endonucleases, Drosha and Dicer, are involved in this process. Primary miRNA is processed by Drosha and precursor miRNA is cleaved by Dicer to produce mature and functional miRNA[9]. The inhibitory function of mature miRNA is mediated by two different pathways: the degradation of mRNA by binding of miRNA to the 3′ untranslated region of mRNA, or direct repression of the translational process[9]. Many biological processes are regulated by miRNA, including cell survival, differentiation and homeostasis; furthermore, specific miRNAs regulate the differentiation of intestinal epithelial cells[10].

Goblet cells are of a secretory epithelial lineage that produces carbohydrate-rich mucus to exclude foreign antigens, including pathogens. Although a published report has shown that intestinal epithelial cell–specific deletion of Dicer1 leads to fewer goblet cells, the miRNA targets or the mechanism by which miRNAs affect these changes were not identified[10]. Biton and colleagues have now used mice with inducible intestinal epithelial cell–specific deficiency in *Dicer1* (*Dicer1*$^{\Delta gut}$) to investigate this[1]. Consistent with the results of the previously published study[10], they find fewer colonic goblet cells in *Dicer1*$^{\Delta gut}$ mice. The authors further identify a specific miRNA, miR-375, that probably inhibits translation of the gene encoding KLF5, an antagonist of the goblet cell–differentiation factor KLF4 (**Fig. 1a**); this therefore suggests that miR-375 probably supports the differentiation of goblet cells by targeting an otherwise repressive transcription factor. In addition, they demonstrate that *Dicer1*$^{\Delta gut}$ mice have lower expression of T_H2 cytokines such as IL-4, IL-5 and IL-13, which leads to enhanced susceptibility to infection caused by the mouse helminth parasite *Trichuris muris*. They also identify IL-13 as a possible cytokine that induces miR-375 in intestinal epithelial cells, at least *in vitro*. They provide evidence that IL-13 induces miR-375, KLF4 upregulation and eventual differentiation of goblet cells (**Fig. 1a**). This IL-13

Yoshiyuki Goto and Hiroshi Kiyono are in the Division of Mucosal Immunology, Department of Microbiology and Immunology, The Institute of Medical Science, The University of Tokyo, Tokyo, Japan.
e-mail: kiyono@ims.u-tokyo.ac.jp

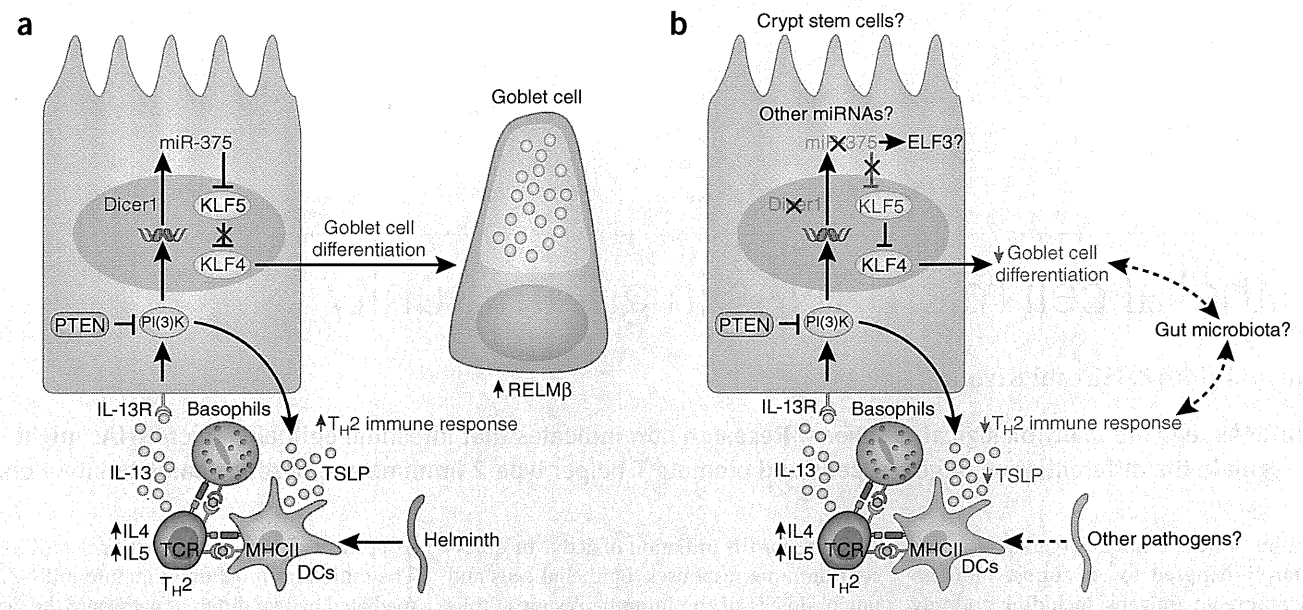

Figure 1 MicroRNAs regulate intestinal epithelial differentiation and T_H2 immune responses. (**a**) Regulation of intestinal innate and acquired immunity by Dicer and miRNA. Dicer1 and miR-375 inhibit KLF5, a known antagonist of KLF4 that promotes the differentiation of goblet cells via KLF4. Helminth infection induces TH2 cytokines, especially IL-13, which leads to epithelial expression of miR-375 and goblet-cell maturation via PI(3)K. Moreover, miR-375 also induces TSLP to accelerate TH2 immune responses to parasite infections. (**b**) Depletion of Dicer1 or miR-375 results in fewer goblet cells and diminished T_H2 responses. On the basis of new findings now reported[1], additional issues have been raised in miRNA-mediated gut immunity. Addressing several unanswered questions will provide fuller understanding of the role of miRNA in establishing optimized mucosal immunity: Does IL-13 directly induce miR-375 in epithelial cells and/or crypt stem cells? Do other miRNAs regulate the differentiation of goblet cells (or other epithelial cells)? Is the gut microbiota involved in the induction and regulation of miRNA expression either for active or quiescent immunity? Are other miRNAs involved in the generation of optimal protective immunity to various pathogens? PTEN, PI(3)K-pathway inhibitory phosphatase; IL-13R, IL-13 receptor; TCR, T cell antigen receptor; MHCII, major histocompatibility complex class II; RELMβ, TH2 antiparasitic cytokine.

is presumably supplied by T_H2 cells because T cell–deficient nude mice have much lower expression of miR-375. Moreover, PI(3)K, a signaling molecule downstream of the IL-13 receptor, mediates miR-375 expression and the differentiation of goblet cells (**Fig. 1a**). IL-13–mediated expression of miR-375, furthermore, leads to TSLP production, which indicates a potential mechanism by which miR-375 could drive an appropriately balanced T_H2 feed-forward loop. On the basis of these results, the authors suggest that the epithelial cell-specific miRNA miR-375 directs the differentiation of goblet cells and the promotion of antiparasitic T_H2 immune responses (**Fig. 1a**). As miR-375 expression is very high in the human intestine[11], mucosal expression of this particular miRNA might also be important in the regulation of intestinal homeostasis and protection against parasite infection in humans.

Several interesting questions are raised by the results reported by Biton *et al.*[1] (**Fig. 1b**). For example, whether the target of miR-375 is solely KLF5 or whether there are other targets relevant to the differentiation of goblet cells and/or gut immunological homeostasis still needs to be clarified. In addition to goblet cell–inducing KLF4, another transcription factor, ELF3, also seems to enhance the differentiation of goblet cells[2]. In support of the contention that other targets may be involved, Biton *et al.* find that deletion of Dicer1 results in more severe impairment of the differentiation of goblet cells than does germline deficiency in miR-375 alone[1]. A more comprehensive analysis of mice with (ideally gut-inducible) knockout of miR-375 or specific antagonism of this miRNA *in vivo* would help delineate its role in gut immunity. It is thus important to elucidate further how miR-375 and probably other miRNAs and their associated targets interact and cooperatively regulate the differentiation of goblet cells.

Goblet cells are constitutively present in normal mice, whereas greater numbers of goblet cells are induced after parasite infection[12]; this suggests that two types of goblet cells develop in the intestinal epithelium: naturally occurring goblet cells and inducible goblet cells. Although ~16% of all epithelial cells in the colon are naturally occurring goblet cells, a limited number of these cells are present in the small intestine, especially the duodenum (~4%)[2]. Although Biton *et al.* find that the differentiation of naturally occurring goblet cells seems to be dependent on miRNA[1], it is possible that IL-13 is a master regulator of this, or that other as-yet-unidentified molecules, including other T_H2-type cytokines, are involved in the differentiation and localization of both types of goblet cell and mucosal expression of miR-375 in the intestine. Moreover, similar to other columnar epithelial cells and endocrine cells, goblet cells are also differentiated from villous crypt stem cells[1]. Does IL-13 produced only by T_H2 cells neighboring crypt stem cells drive miR-375 expression and subsequent differentiation of goblet cells, or do dispersed T_H2 cells and/or other subsets of T cells also have such functions involving epithelial miRNA–mediated cell differentiation and immunity? Answering these questions will help elucidate how miRNAs direct the differentiation of crypt stem cells and the specificity of the miRNAs required for intestinal homeostasis.

During parasite infection, one of the main immunologically relevant functions of epithelial miRNA seems to be TSLP induction and the promotion of T_H2 responses (**Fig. 1a**). In addition to the differentiation of goblet cells, which seems to skew toward T_H2 antiparasitic immune responses, whether other epithelial miRNAs regulate T_H1 and/or T_H2 responses requires further analysis. In addition, defective mucous secretion caused by goblet cell hypoplasia could lead to aberrant

composition and localization of the gut microflora and thereby diminish mucosal T_H2 responses (**Fig. 1b**). It will therefore be important to examine whether the gut microbiota regulates intestinal miRNAs involved in the development of mucosal homeostasis (**Fig. 1b**). The role of mucosa-associated miRNA in the differentiation of epithelial cells and regulation of the mucosal immune system is only just beginning to be explored. Further investigation should open the door to the development of innovative mucosal miRNA–targeted treatments and the diagnosis of pathogenic mucosal conditions such as allergy, inflammatory bowel diseases and colon cancer, as well as infection by bacteria, viruses and parasites.

COMPETING FINANCIAL INTERESTS
The authors declare no competing financial interests.

1. Biton, M. *et al. Nat. Immunol.* **12**, 239–246 (2011).
2. van der Flier, L.G. & Clevers, H. *Annu. Rev. Physiol.* **71**, 241–260 (2009).
3. Rimoldi, M. *et al. Nat. Immunol.* **6**, 507–514 (2005).
4. Dahan, S., Roth-Walter, F., Arnaboldi, P., Agarwal, S. & Mayer, L. *Immunol. Rev.* **215**, 243–253 (2007).
5. Atarashi, K. *et al. Science* **331**, 337–341 (2011).
6. Gaboriau-Routhiau, V. *et al. Immunity* **31**, 677–689 (2009).
7. Ivanov, I.I. *et al. Cell* **139**, 485–498 (2009).
8. Maizels, R.M., Pearce, E.J., Artis, D., Yazdanbakhsh, M. & Wynn, T.A. *J. Exp. Med.* **206**, 2059–2066 (2009).
9. Bartel, D.P. *Cell* **116**, 281–297 (2004).
10. McKenna, L.B. *et al. Gastroenterology* **139**, 1654–1664, (2010).
11. Wu, F. *et al. Inflamm. Bowel Dis.* **16**, 1729–1738 (2010).
12. Ishikawa, N. *et al. Gastroenterology* **113**, 542–549 (1997).

AIDing the pursuit of IgA diversity

Kang Chen & Andrea Cerutti

Direct evaluation of the contribution of somatic hypermutation (SHM) to mucosal immunity has been hampered by the lack of models able to dissociate SHM from class-switch recombination, which are both dependent on the cytidine deaminase AID. A new mouse AID model now demonstrates the critical role of SHM in the control of gut bacteria.

The diversification of immunoglobulin genes is critical for the generation of immune protection. This is particularly true at mucosal sites such as the intestine, which is populated by a large community of commensal bacteria. Mature B cells generate immunoglobulin gene diversity by undergoing somatic hypermutation (SHM) and class-switch recombination (CSR) in the germinal center of lymphoid follicles. SHM introduces point mutations into recombined variable-diversity-joining (V(D)J) exons that encode the antigen-binding V region of immunoglobulins, thereby providing the structural correlate for the selection of high-affinity immunoglobulin mutants by antigen[1]. In contrast, CSR replaces the μ-chain constant region (C_μ) exon, which encodes immunoglobulin M (IgM), with C_γ, C_α or C_ε exons, which encode IgG, IgA or IgE, thereby providing immunoglobulins with new effector functions without changing their specificity for antigen[1]. Both SHM and CSR require the DNA-editing enzyme AID (activation-induced cytidine deaminase)[2]. Because of this common reliance on AID and hence the difficulty in dissociating SHM from CSR in mice that lack AID, the specific contribution of SHM to mucosal immunity has remained elusive. In this issue of *Nature Immunology*, Wei *et al.* use a mouse model that expresses an SHM-defective but CSR-competent AID molecule to show that SHM is critical for the generation of homeostasis and immunity in the intestine by B cells[3].

The interaction between the intestinal mucosa and commensals has been in the limelight in the past decade because of its huge relevance to the biology of both health and disease states. It is now well recognized that commensals establish a symbiotic relationship with the host in the intestine, as they process otherwise indigestible food components, synthesize essential vitamins, stimulate the maturation of the immune system, and form an ecological niche that restricts the growth of pathogenic species[4]. Conversely, the host provides commensals with a habitat rich in energy derived from the processing

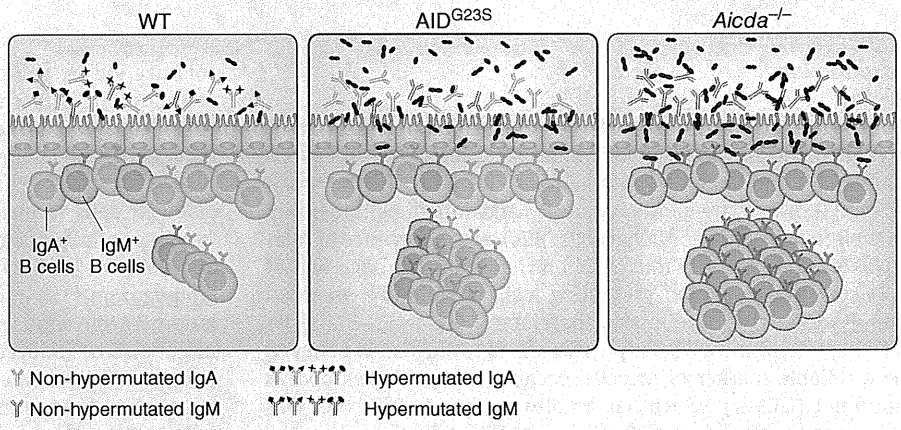

Figure 1 Lack of SHM impairs mucosal homeostasis and immunity. In wild-type (WT) mice (left), AID-mediated antibody diversification via CSR and SHM generates a diversified mucosal repertoire comprising IgA (green) and, to a lesser extent, IgM (blue), which regulates the composition of the local commensal microbiota. Mice expressing the CSR-competent but SHM-defective mutant AIDG^{23S} molecule (middle) produce normal amounts of unmutated IgA and IgM, which cannot efficiently recognize the intestinal microflora, thereby causing aberrant expansion of and more epithelial adhesion of certain bacterial species. More penetration of these bacteria across the epithelial barrier drives the hyperactivation of mucosal lymphoid follicles, including Peyer's patches. Similar but more profound abnormalities are present in AID-deficient (*Aicda*$^{-/-}$) mice (right), which show profound defects in both CSR and SHM and hence express only unmutated IgM.

Kang Chen is with The Immunology Institute, Mount Sinai School of Medicine, New York, New York, USA. Andrea Cerutti is with The Immunology Institute, Mount Sinai School of Medicine, New York, New York, USA, and the Catalan Institute for Research and Advanced Studies, L'Institut Municipal d'Investigació Mèdica Hospital del Mar, Barcelona Biomedical Research Park, Barcelona, Spain.
e-mail: acerutti@imim.es

Biochemical and Biophysical Research Communications 404 (2011) 822–828

Contents lists available at ScienceDirect

Biochemical and Biophysical Research Communications

journal homepage: www.elsevier.com/locate/ybbrc

Distinct fucosylation of M cells and epithelial cells by Fut1 and Fut2, respectively, in response to intestinal environmental stress

Kazutaka Terahara [a], Tomonori Nochi [b], Masato Yoshida [b], Yuko Takahashi [b], Yoshiyuki Goto [b], Hirotsugu Hatai [b], Shiho Kurokawa [b], Myoung Ho Jang [c], Mi-Na Kweon [d], Steven E. Domino [e], Takachika Hiroi [f], Yoshikazu Yuki [b], Yasuko Tsunetsugu-Yokota [a], Kazuo Kobayashi [a], Hiroshi Kiyono [b,*]

[a] Department of Immunology, National Institute of Infectious Diseases, 1-23-1 Toyama, Shinjuku-ku, Tokyo 162-8640, Japan
[b] Division of Mucosal Immunology, Department of Microbiology and Immunology, The Institute of Medical Science, The University of Tokyo, 4-6-1 Shirokanedai, Minato-ku, Tokyo 108-8639, Japan
[c] Laboratory of Gastrointestinal Immunology, World Premier International Immunology Frontier Research Center, Osaka University, 3-1 Yamada-oka, Suita, Osaka 565-0871, Japan
[d] Mucosal Immunology Section, International Vaccine Institute, Seoul 151-818, Republic of Korea
[e] Department of Obstetrics and Gynecology, The University of Michigan Medical School, 6428 Medical Science Bldg I, 1150 West Medical Center Drive, Ann Arbor, MI 48109-5617, USA
[f] Department of Allergy and Immunology, The Tokyo Metropolitan Institute of Medical Science, 2-1-6 Kamikitazawa, Setagaya-ku, Tokyo 156-8506, Japan

ARTICLE INFO

Article history:
Received 13 December 2010
Available online 21 December 2010

Keywords:
Epithelial cell
Fucosyltransferase
Intestine
M cell
Peyer's patch

ABSTRACT

The intestinal epithelium contains columnar epithelial cells (ECs) and M cells, and fucosylation of the apical surface of ECs and M cells is involved in distinguishing the two populations and in their response to commensal flora and environmental stress. Here, we show that fucosylated ECs (F-ECs) were induced in the mouse small intestine by the pro-inflammatory agents dextran sodium sulfate and indomethacin, in addition to an enteropathogen derived cholera toxin. Although F-ECs showed specificity for the M cell-markers, lectin *Ulex europaeus* agglutinin-1 and our monoclonal antibody NKM 16-2-4, these cells also retained EC-phenotypes including an affinity for the EC-marker lectin wheat germ agglutinin. Interestingly, fucosylation of Peyer's patch M cells and F-ECs was distinctly regulated by α(1,2)fucosyltransferase Fut1 and Fut2, respectively. These results indicate that Fut2-mediated F-ECs share M cell-related fucosylated molecules but maintain distinctive EC characteristics, Fut1 is, therefore, a reliable marker for M cells.

1. Introduction

M cells are generally observed in the follicle-associated epithelium (FAE) of mucosa-associated lymphoid tissues including Peyer's patches (PPs) and isolated lymphoid follicles (ILFs) in the small intestine [1,2], and are morphologically and functionally distinct from their neighboring epithelial cells (ECs) by the presence of relatively short and irregular microvilli on their apical surface and of lymphocytes and antigen-presenting cells frequently enfolded within a pocket structure in their basolateral region [3–5]. In the small intestine of mice, the expression of α(1,2)fucose is believed to be a reliable marker of M cells, because lectin *Ulex europaeus* agglutinin-1 (UEA-1), which has an affinity for α(1,2)fucose, was found to bind exclusively to M cells in the PPs [6,7]. Subsequently, we could found M cells located within the non-FAE-associated small intestinal villous epithelium by utilizing an affinity of UEA-1 [8].

Interestingly, α(1,2)fucosylation is also induced in ileal villous ECs by a variety of intestinal environmental stresses (IES) such as colonization by commensal bacteria, weaning, mechanical injury or treatment with chemicals inhibiting protein synthesis [9–11]. When considering the possible involvement of IES in the development of (or conversion to) M cells, it is reasonable to postulate that such fucosylated ECs form a subset of M cells, because the number of PP M cells is increased rapidly and transiently by alteration from specific pathogen-free (SPF) conditions to a conventional environment [12], by interaction with bacteria such as *Salmonella typhimurium* [13] and *Streptococcus pneumoniae* [14] and during indomethacin-induced ileitis [15]. Like PP M cells, villous M cells might also be induced (or converted) by IES, because a higher frequency of villous M cells is observed in the terminal ileum, which is enriched for commensal bacteria [16]. Recently, we found that some ECs underwent α(1,2)fucosylation in the small intestinal villous epithelium when a mucosal adjuvant cholera toxin (CT) derived from a well known enteropathogen *Vibrio cholerae* was orally administered into mice, and that these cells, in part, shared the same gene expression profile as PP M cells; we previously designated them "M-like cells" [17].

In mice, α(1,2)fucosyltransferase Fut1 and Fut2 are the enzymes responsible for catalyzing an α(1,2) linkage of fucose to terminal β-galactoside, and Fut2 is involved in the IES-associated fucosylation

* Corresponding author. Fax: +81 3 5449 5411.
E-mail address: kiyono@ims.u-tokyo.ac.jp (H. Kiyono).

0006-291X/$ - see front matter © 2010 Elsevier Inc. All rights reserved.
doi:10.1016/j.bbrc.2010.12.067

whereas little is known about Fut1 in the intestine [11,18–20]. In this study, we aimed to elucidate the biological characteristics of ECs that shared the α(1,2)fucose modification with M cells focusing on the fucosylation mechanism, in the hope of better understanding of whether ECs can be reprogrammed into M (or M-like) cells in response to IES.

2. Materials and methods

2.1. Mice

BALB/c and C57BL/6J mice were purchased from SLC (Shizuoka, Japan). Fut1-null and Fut2-null mice (C57BL/6J background) were generated as previously described [21]. These mice were maintained under SPF conditions and used in experiments at 6–9 weeks old. All animal experiments were approved by the Animal Care and Use Committee of The University of Tokyo.

2.2. Lectins and antibodies

The following lectins and antibodies were used for flow cytometry (FCM) and confocal laser scanning microscopy (CLSM): PE-conjugated UEA-1 (UEA-1-PE; Biogenesis, England, UK), tetramethylrhodamine isothiocyanate (TRITC)-conjugated UEA-1 (Vector Laboratories, Burlingame, CA), Alexa Fluor 633-conjugated wheat germ agglutinin (WGA-AF633; Molecular Probes, Eugene, OR), FITC-conjugated NKM 16-2-4 mAb (NKM 16-2-4-FITC) [22], APC-conjugated anti-mouse CD45 mAb (anti-CD45-APC; BD Biosciences, San Jose, CA).

2.3. Alteration of the intestinal environment

A mucosal adjuvant, CT (List Biologic Laboratories, Campbell, CA), and two pro-inflammatory agents, dextran sodium sulfate (DSS, m.w. 36,000–50,000; ICN Biomedicals, Irvine, CA) and indomethacin (Sigma–Aldrich, St. Louis, MO), were used as stress-inducing agents to alter the intestinal environment of mice as described previously [17,23,24] (see Supplementary information).

2.4. Preparation of intestinal epithelial cells for FCM

The small intestinal epithelium was dissociated by a mechanical procedure as described previously [17]. The mononuclear cells were stained with NKM 16-2-4-FITC, UEA-1-PE and anti-CD45-APC and dead cells were stained with 7-aminoactinomycin D (BD Biosciences). Fluorescently labeled cells were analyzed and, if necessary, sort-purified using a FACSAria flow cytometer (BD Biosciences) (see Supplementary information).

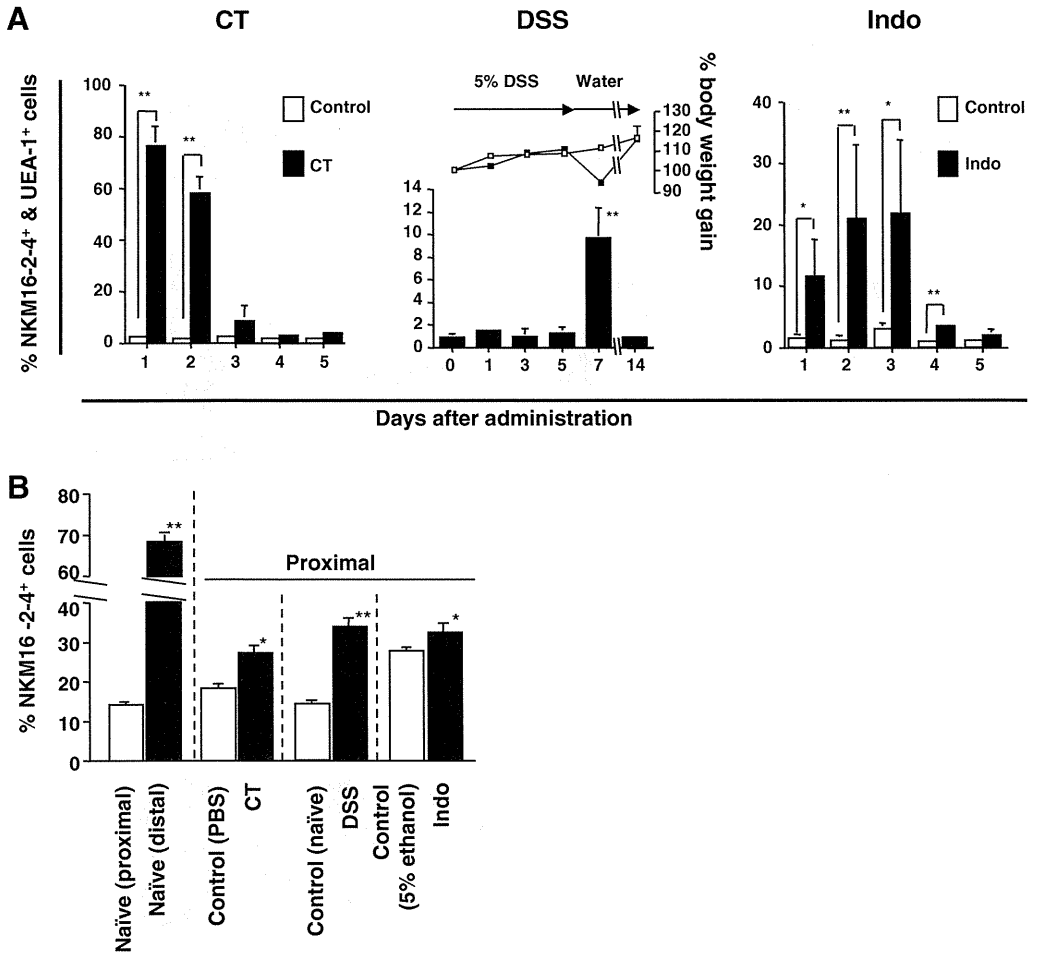

Fig. 1. The influence of IES on the induction of α(1,2)fucosylation in the small intestinal epithelia of BALB/c mice. (A) Daily analysis of the frequency of NKM 16-2-4$^+$/UEA-1$^+$ cells in the proximal villous epithelium of CT-, DSS- and indomethacin (Indo)-administered mice based on FCM. The ratio of NKM 16-2-4$^+$/UEA-1$^+$ cells was enumerated in cells, with 7-aminoactinomycin D$^+$ dead cells, CD45$^+$ leukocytes and small forward- and side-scattered lymphocytes gated out. The line graph in the middle panel shows the percentage body weight gain of control (open squares) and DSS-administered (filled squares) mice. Data are given as means ± SE (n = 3–7). Significant differences ($^*P < 0.05$, $^{**}P < 0.01$) were determined by t-test or Mann–Whitney's U test. (B) The proportions of NKM 16-2-4$^+$ cells in the PP domes based on histoplanimetrical analysis of CLSM images. Mice used were naïve, or were administered CT (day 1), DSS (day 7) or Indo (day 1). Data are given as means ± SE (n = 3, 19–76 domes). Significant differences ($^*P < 0.05$, $^{**}P < 0.01$) were determined by t-test.

2.5. Histological analysis

Fluorescently labeled whole-mount tissues were analyzed by CLSM as described previously [8,22]. Each area of NKM 16-2-4$^+$ cells and whole FAE in PPs was quantitated using Scion Image software (Scion Corporation, Frederick, MA) based on the data obtained by CLSM (see Supplementary information).

2.6. Quantitative real-time RT-PCR for Fut1 and Fut2 transcripts

The levels of the *Fut1* and *Fut2* transcripts were quantitated by real-time RT-PCR in the cDNA samples from the sorted cells with reference to the level of hypoxanthine guanine phosphoribosyl transferase (*Hprt*) transcripts (see Supplementary information).

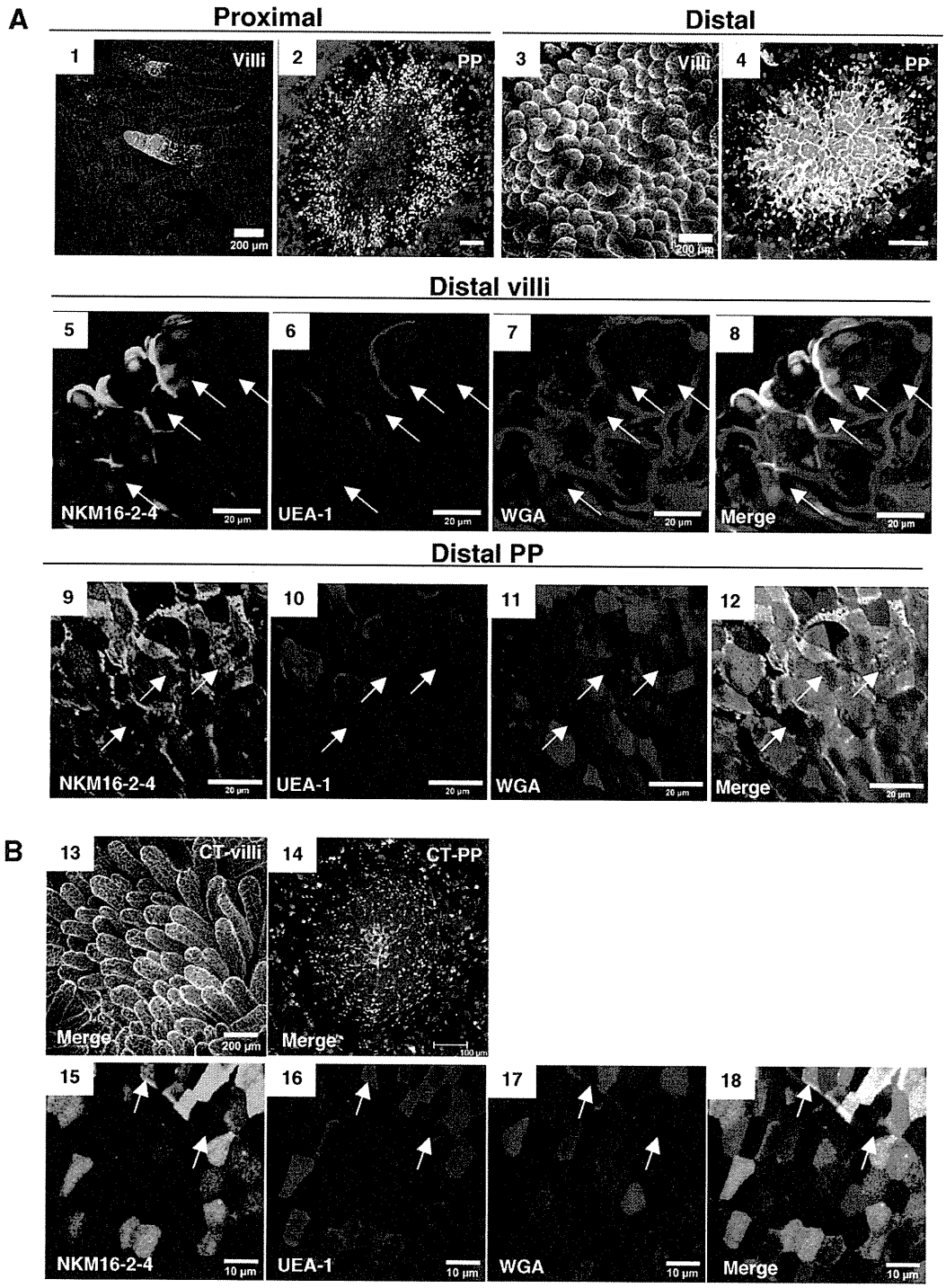

Fig. 2. CLSM analysis of whole-mount small intestinal epithelia of BALB/c mice. Confocal images stained with NKM 16-2-4-FITC, UEA-1-TRITC and WGA-AF633 are shown by green, red and blue, respectively. (A) Proximal villi (1) and PP (2), and distal villi (3, 5–8) and PP (4, 9–12) from naïve mice. (B) Proximal villi (13, 15–18) and PP (14), 1 day after oral CT administration. Arrows show villous M cells (NKM 16-2-4$^+$/UEA-1$^+$/WGA$^-$). Scale bars are 200 μm (1, 3, 13), 100 μm (2, 4, 14), 20 μm (5–12) or 10 μm (15–18). (For interpretation of the references to colour in this figure legend, the reader is referred to the web version of this article.)

2.7. Statistical analysis

The significance of the data was evaluated by the unpaired *t*-test, Mann–Whitney's U test, Tukey's or Scheffé's multiple comparison test based on the normality and variance of the data compared using Statcel2 software (OMS Publishing Inc., Saitama, Japan). $P < 0.05$ was considered statistically significant.

3. Results

3.1. Induction of α(1,2)fucosylation in the small intestinal epithelium by IES

To examine the influence of IES on M cell-associated α(1,2)fucosylation (NKM 16-2-4$^+$/UEA-1$^+$), we focused on the proximal epithelium, where NKM 16-2-4$^+$/UEA-1$^+$ cells were rarely found in naïve mice (Supplementary Fig. S1). When CT was orally administered to BALB/c mice, NKM 16-2-4$^+$/UEA-1$^+$ cells were dramatically increased in the proximal villous epithelium, with an average of 75.9% double-positive cells one day post-inoculation (Fig. 1A). The proportion of NKM 16-2-4$^+$/UEA-1$^+$ cells returned to the control level (approximately 2%) at 3 days post-inoculation. Similarly, a significant increase in NKM 16-2-4$^+$/UEA-1$^+$ cells was observed when pro-inflammatory agents, such as DSS or indomethacin, were administered (Fig. 1A).

A similar tendency was also seen in the FAE of PPs. We next performed histoplanimetrical analysis based on single NKM 16-2-4 signals obtained by CLSM. We previously demonstrated that NKM 16-2-4$^+$ cells included UEA-1$^+$ M cells but not goblet cells [22]. However, similar to UEA-1, because NKM 16-2-4 reacts to Paneth cells (Supplementary Fig. S2), NKM 16-2-4$^+$ cells were enumerated upward the crypts where Paneth cells locally exist. Therefore, goblet cells and Paneth cells were excluded in this analysis. When the proportions of NKM 16-2-4$^+$ cells were compared between the proximal and distal PP FAE of naïve BALB/c mice, a higher frequency of NKM 16-2-4$^+$ cells was observed in the distal (68.4%) than in the proximal (13.9%) PP FAE (Fig. 1B). Furthermore, a significant increase in NKM 16-2-4$^+$ cells was observed in the proximal PP FAE following CT-, DSS- or indomethacin-administration, averaging 27.2% (control: 18.1%), 33.8% (control: 13.9%) and 32.4% (control: 27.5%) positive cells, respectively (Fig. 1B). These results indicate that IES enhances α(1,2)fucosylation in both the PP FAE and the villous epithelium.

3.2. CLSM analysis of IES-induced NKM 16-2-4$^+$/UEA-1$^+$ cells

To assess qualitative cellular traits of IES-induced NKM 16-2-4$^+$/UEA-1$^+$ cells, we performed CLSM analysis using lectin WGA, which has an affinity for ECs and goblet cells but not M cells [6,8]. As indicated by FCM (Supplementary Fig. S1), a higher frequency of NKM 16-2-4$^+$/UEA-1$^+$ cells was observed in the distal (Fig. 2A; 3 and 4) than in the proximal villi and PPs (Fig. 2A; 1 and 2) in naïve BALB/c mice. In general, these NKM 16-2-4$^+$/UEA-1$^+$ cells were preferentially located at the tips of the villi (Fig. 2A; 1 and 3) and PP domes (Fig. 2A; 4) and a large proportion of them showed an affinity for WGA in both the villous epithelium (Fig. 2A; 7) and the PP FAE (Fig. 2A; 11), although a substantial number of villous M cells sharing the typical M cell hallmark (NKM 16-2-4$^+$/UEA-1$^+$/WGA$^-$) existed in the distal villi of naïve mice (Fig. 2A; 5–8: arrows).

The CLSM analysis further demonstrated that CT-induced NKM 16-2-4$^+$/UEA-1$^+$ cells also reacted with WGA (Fig. 2B). In contrast, villous M cells showing the M cell-phenotype (NKM 16-2-4$^+$/UEA-1$^+$/WGA$^-$) remained at a very low frequency irrespective of IES by CT (Fig. 2B; 15–18: arrows). A similar observation was made when DSS or indomethacin was administered (Supplementary Fig. S3). In the proximal PP FAE, whereas a substantial number of NKM 16-2-4$^+$/UEA-1$^+$ cells were negative for WGA and were radially distributed on the dome, indicating an M cell-phenotype (Fig. 2A; 2), triple-positive cells (NKM 16-2-4$^+$/UEA-1$^+$/WGA$^+$) were evident and were located on the tip of the dome after oral CT administration (Fig. 2B; 14). These results indicate that IES-induced NKM 16-2-4$^+$/UEA-1$^+$ cells share an affinity for WGA, a common trait of normal ECs [6], and hardly contain any villous M cells. We thus designated them fucosylated ECs (F-ECs), to distinguish them from typical M cells.

3.3. Different expression patterns of Fut1 and Fut2 transcripts in the small intestinal epithelium

To examine in more detail the mechanism of α(1,2)fucosylation between F-ECs and M cells, we performed quantitative real-time RT-PCR for *Fut1* and *Fut2* transcripts. Quantitative real-time RT-PCR demonstrated that high expression of *Fut1* transcripts was seen only in NKM 16-2-4$^+$/UEA-1$^+$ cells isolated from the naïve PP FAE where M cells predominantly exist (Fig. 3A). On the other hand, elevated expression of *Fut2* transcripts, but not *Fut1* transcripts, was detected in F-ECs located in the distal epithelia of naïve mice (Fig. 3A and B). Similarly, enhanced expression of *Fut2* transcripts, but not *Fut1* transcripts, was seen in CT-, DSS- and indomethacin-induced F-ECs of the proximal epithelia (Fig. 3A and B). These results indicate that α(1,2)fucosylation of F-ECs in the villous epithelium is induced by Fut2, and suggest that Fut1 is expressed in PP M cells irrespective of IES.

3.4. Distinct requirements for Fut1 or Fut2 for α(1,2)fucosylation of M cells or F-ECs, respectively

To clarify the distinct requirements for the Fut isoforms in F-ECs and M cells, Fut1-null and Fut2-null mice were employed for FCM

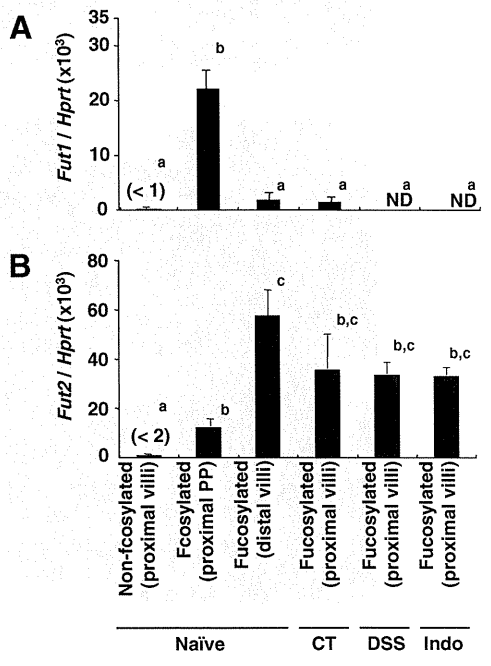

Fig. 3. Quantification of the expression levels of *Fut1* and *Fut2* transcripts relative to levels of *Hprt* transcripts. Fucosylated (NKM 16-2-4$^+$/UEA-1$^+$) and non-fucosylated (UEA-1$^-$) cells were purified from the proximal or distal small intestinal epithelia using a cell-sorter. Naïve, or CT- (Day 2), DSS- (Day 7) or indomethacin (Indo)- (Day 2) treated BALB/c mice were used. (A) *Fut1* transcripts. (B) *Fut2* transcripts. Data are given as means ± SE ($n = 3$–4). Different letters indicate significant differences ($P < 0.05$) determined by Tukey's multiple comparison test.

and CLSM analyses. Because these mice are on a C57BL/6J background [21], wild-type (WT) C57BL/6J mice were employed as a control group. Like BALB/c mice, WT C57BL/6J mice showed a higher frequency of F-ECs (NKM 16-2-4$^+$/UEA-1$^+$ cells) in the distal villous epithelium than in the proximal villous epithelium, and that the frequency of F-ECs in the latter increased after oral CT administration (Fig. 4A). This was also observed when Fut1-null mice were orally exposed to CT (Fig. 4A and C; 2 and 4). On the

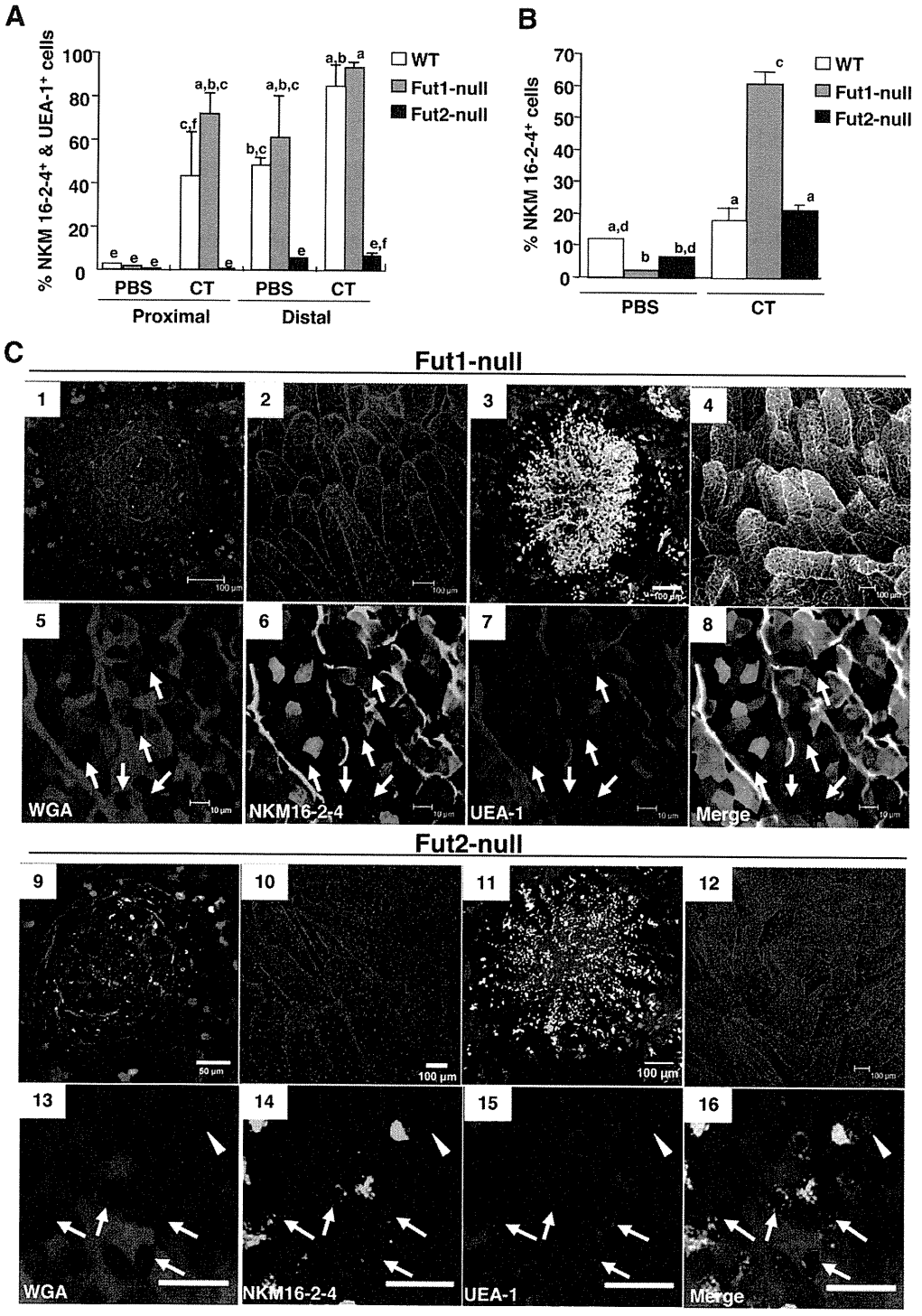

Fig. 4. Fut1- and Fut2-dependent α(1,2)fucosylation in PP M cells and F-ECs, respectively. (A) The proportions of NKM 16-2-4$^+$/UEA-1$^+$ cells in the proximal and distal villous epithelia of either day 1 PBS- or CT-administered (CT) WT C57BL/6J, Fut1-null and Fut2-null mice based on FCM as described in the Fig. 1 legend. Data are given as means ± SE ($n = 3$). Different letters indicate significant differences ($P < 0.05$) determined by Tukey's multiple comparison test. (B) The proportions of NKM 16-2-4$^+$ cells in the proximal PP domes based on histoplanimetrical analysis of CLSM images. WT, Fut1-null and Fut2-null mice were used after oral administration of either PBS or CT (day 1). Data are given as means ± SE ($n = 3$, 12–25 domes). Different letters indicate significant differences ($P < 0.05$) determined by Scheffé's multiple comparison test. (C) CLSM analysis for the whole-mount small intestinal epithelia of either naïve or day 1 CT-treated Fut1-null (naïve; 1, 2, CT; 3–8) and Fut2-null mice (naïve; 9, 10, CT; 11–16). Confocal images stained with NKM 16-2-4-FITC, UEA-1-TRITC and WGA-AF633 are shown by green, red and blue, respectively. Arrows and arrowheads indicate WGA$^-$ PP M cells and Fut1-dependent WGA$^+$ cells, respectively. Scale bars are 100 μm (1–4, 10–12), 50 μm (9), 20 μm (13–16) or 10 μm (5–8). (For interpretation of the references to colour in this figure legend, the reader is referred to the web version of this article.)

other hand, Fut2-null mice possessed few NKM 16-2-4$^+$/UEA-1$^+$ cells in the villous epithelia and the number of these cells was not increased upon oral CT administration (Fig. 4A and C; 10 and 12). PBS-administered Fut2-null mice showed 0.1% and 4.9% of NKM 16-2-4$^+$/UEA-1$^+$ cells in the proximal and distal villous epithelia, respectively, and CT-administered Fut2-null mice showed 0.3% and 5.3% in the proximal and distal villous epithelia, respectively (Fig. 4A).

In contrast to the villous epithelia, the PP FAE contained both types of fucosylated cells, dependent on either Fut1 or Fut2. In PBS-administered conditions, 2.0% and 6.3% of NKM 16-2-4$^+$ cells were observed in the proximal PP FAE of Fut1-null and Fut2-null mice, respectively (Fig. 4B). Oral CT administration did not notably induce α(1,2)fucosylation in the PP FAE of WT mice; CT-administered and PBS-administered WT mice contained 17.8% and 12.0% of NKM 16-2-4$^+$ cells, respectively, and there was no statistical difference between the two groups (Fig. 4B). However, both Fut1-null and Fut2-null mice showed significant induction of NKM 16-2-4$^+$ cells in the proximal PP FAE, with the proportion of positive cells being 60.5% and 21.0%, respectively (Fig. 4B). CLSM analysis further revealed that the fucosylation of M cells was dependent on Fut1, because WGA$^-$ M cells did not induce α(1,2)fucosylation and thus did not react with either NKM 16-2-4 or UEA-1 in Fut1-null mice (Fig. 4C; 1, 3 and 5–8: arrows) whereas they did react with these markers in Fut2-null mice (Fig. 4C; 9, 11 and 13–16: arrows) irrespective of oral CT administration. In addition, the fucosylation of F-ECs in the PP FAE was dependent on Fut2 because triple-positive cells (NKM 16-2-4$^+$/UEA-1$^+$/WGA$^+$ cells) were preferentially observed in the CT-administered Fut1-null mice (Fig. 4C; 3 and 5–8). Although a small number of Fut1-dependent WGA$^+$ cells were observed in the PP FAE of CT-administered Fut2-null mice (Fig. 4C; 13–16: arrowheads), they were distributed radially, accompanying abundant WGA$^-$ M cells on the PP dome (Fig. 4C; 11), and were distinguishable from the Fut2-dependent F-ECs that were distributed all over the dome (Fig. 4C; 3).

Taken together, these results indicate that α(1,2)fucosylation of PP M cells is dependent on Fut1 irrespective of IES, and that Fut2 is involved in α(1,2)fucosylation of F-ECs residing in both the PP FAE and villous epithelium in response to IES.

4. Discussion

In this study, we showed that intestinal environmental and biological stress induced F-ECs, which were recognized by NKM 16-2-4 and UEA-1, in both the PP FAE and the villous epithelium. However, such IES-induced F-ECs possessed a strong affinity for WGA (Fig. 2). In addition, F-ECs showed the same morphological characteristics as ECs such as columnar architecture, well-developed tall and dense microvilli (Supplementary Fig. S4), and did not possess *Salmonella* uptake-ability (Supplementary Fig. S5). Furthermore, F-ECs did not express glycoprotein 2 (Supplementary Fig. S6 and Table S1), recently identified as an M cell-specific molecule [17,25]. Therefore, F-ECs should be distinguished from typical M cells, and IES-induced α(1,2)fucosylation reflects only a phenotypic change of surface glycosylation pattern that is irrelevant to M-cell differentiation.

The requirements for different fucosylation-inducing enzymes clearly demonstrated a distinction between F-ECs and PP M cells: Fut1 is essential for the fucosylation associated with PP M cells while Fut2 is specifically involved in the fucosylation of IES-induced F-ECs in both the PP FAE and villous epithelium (Fig. 4). Although it has been reported that the expression of *Fut1* transcripts is rare and is not induced or altered in the small intestine by the transfer from germ-free to conventional conditions [11,18–20], these results are probably due to the low frequency of PP M cells throughout the small intestine. In contrast, it has been known that *Fut2* transcripts are induced in the small intestine, particularly in the ileum, of mice in response to colonization by commensal bacteria or treatment with a protein synthesis inhibitor [11,19]. Our present data, in which IES resulted in the induction of Fut2-dependent F-ECs, is consistent with and support these previous findings.

Fut1 and Fut2 provide insights into the involvement of IES in the development of not only F-ECs but also M cells. The PP dome epithelium consists of two cell lineages: one is derived from the dome-associated crypts and differentiates into either M cells or ECs, and the other is derived from villus-associated crypts and differentiates into ECs [26]. In addition, some studies have revealed a dynamic and plastic morphology of M cells; for example, the distinctive microfold and membranous structures occur transiently during the cell differentiation process, and M cell-lineage cells in their early and terminal development stages show the same morphological structure as ECs [27,28]. In this study, we showed a possibility that Fut1-dependent fucosylated cells are increased by IES (Fig. 4). These cells consisted of abundant PP M cells and a few WGA$^+$ EC-like cells, both of which were distributed radially on the dome. To this end, we suggest a possibility that Fut1-dependent cells are M cell-lineage cells derived from the dome-associated crypts that participate in the increase of M cells in response to IES, as described elsewhere [12–15]. In contrast to PP M cells, the fucosylation of villous M cells, like F-ECs, is regulated by Fut2 because α(1,2)fucosylation in the villi was not observed in Fut2-null but Fut1-null mice regardless of oral CT administration (Fig. 4 and Supplementary Table S1). However, IES alone would not influence the frequency of villous M cells because oral CT administration did not induce *Salmonella* uptake in the villi (Supplementary Fig. S5). It has recently been shown that receptor activator of nuclear factor-kappa B ligand (RANKL) is capable of the full development of both PP and villous M cells but RANKL-expressing inducer cells preferentially exist in the subepithelial dome of PPs [29]. Taken together, transient IES alone might be insufficient for the recruitment and/or induction of RANKL-expressing cells in the villi, and/or other factors might be required for the full development of villous M cells.

Although specific functions of F-ECs remain to be elucidated, our present study offers the possibility that Fut1-null and Fut2-null mice would provide a direct opportunity to examine *in vivo* the immuno-biological role of F-ECs and M cells, including their specific fucosylated glycans, towards a better understanding of the gut mucosal immune system.

Acknowledgments

We thank Dr. Osamu Igarashi for technical support and Dr. Rebecca Devon for editing the manuscript. This work was supported in part by Grants from the Ministry of Education, Science, Sports and Culture of Japan (H.K. and K.T.), and the Ministry of Health, Labour and Welfare of Japan (H.K.).

Appendix A. Supplementary data

Supplementary data associated with this article can be found, in the online version, at doi:10.1016/j.bbrc.2010.12.067.

References

[1] M.R. Neutra, A. Frey, J.P. Kraehenbuhl, Epithelial M cells: gateways for mucosal infection and immunization, Cell 86 (1996) 345–348.
[2] H. Hamada, T. Hiroi, Y. Nishiyama, et al., Identification of multiple isolated lymphoid follicles on the antimesenteric wall of the mouse small intestine, J. Immunol. 168 (2002) 57–64.
[3] R.L. Owen, A.L. Jones, Epithelial cell specialization within human Peyer's patches: an ultrastructural study of intestinal lymphoid follicles, Gastroenterology 66 (1974) 189–203.

[4] M.R. Neutra, N.J. Mantis, A. Frey, et al., The composition and function of M cell apical membranes: implications for microbial pathogenesis, Semin. Immunol. 11 (1999) 171–181.
[5] J.P. Kraehenbuhl, M.R. Neutra, Epithelial M cells: differentiation and function, Annu. Rev. Cell Dev. Biol. 16 (2000) 301–332.
[6] M.A. Clark, M.A. Jepson, N.L. Simmons, et al., Differential expression of lectin-binding sites defines mouse intestinal M-cells, J. Histochem. Cytochem. 41 (1993) 1679–1687.
[7] M.A. Clark, M.A. Jepson, N.L. Simmons, et al., Selective binding and transcytosis of Ulex europaeus 1 lectin by mouse Peyer's patch M-cells in vivo, Cell Tissue Res. 282 (1995) 455–461.
[8] M.H. Jang, M.N. Kweon, K. Iwatani, et al., Intestinal villous M cells: an antigen entry site in the mucosal epithelium, Proc. Natl. Acad. Sci. USA 101 (2004) 6110–6115.
[9] Y. Umesaki, M. Ohara, Factors regulating the expression of the neutral glycolipids in the mouse small intestinal mucosa, Biochim. Biophys. Acta 1001 (1989) 163–168.
[10] L. Bry, P.G. Falk, T. Midtvedt, et al., A model of host-microbial interactions in an open mammalian ecosystem, Science 273 (1996) 1380–1383.
[11] B. Lin, Y. Hayashi, M. Saito, et al., GDP-fucose: beta-galactoside alpha1,2-fucosyltransferase, MFUT-II, and not MFUT-I or -III is induced in a restricted region of the digestive tract of germ-free mice by host-microbe interactions and cycloheximide, Biochim. Biophys. Acta 1487 (2000) 275–285.
[12] M.W. Smith, P.S. James, D.R. Tivey, M cell numbers increase after transfer of SPF mice to a normal animal house environment, Am. J. Pathol. 128 (1987) 385–389.
[13] T.C. Savidge, M.W. Smith, P.S. James, et al., Salmonella-induced M-cell formation in germ-free mouse Peyer's patch tissue, Am. J. Pathol. 139 (1991) 177–184.
[14] C. Borghesi, M.J. Taussig, C. Nicoletti, Rapid appearance of M cells after microbial challenge is restricted at the periphery of the follicle-associated epithelium of Peyer's patch, Lab. Invest. 79 (1999) 1393–1401.
[15] T. Kucharzik, A. Lugering, N. Lugering, et al., Characterization of M cell development during indomethacin-induced ileitis in rats, Aliment. Pharmacol. Ther. 14 (2000) 247–256.
[16] J. Mach, T. Hshieh, D. Hsieh, et al., Development of intestinal M cells, Immunol. Rev. 206 (2005) 177–189.
[17] K. Terahara, M. Yoshida, O. Igarashi, et al., Comprehensive gene expression profiling of Peyer's patch M cells, villous M-like cells and intestinal epithelial cells, J. Immunol. 180 (2008) 7840–7846.
[18] S.E. Domino, N. Hiraiwa, J.B. Lowe, Molecular cloning, chromosomal assignment and tissue-specific expression of a murine alpha(1,2)-fucosyltransferase expressed in thymic and epididymal epithelial cells., Biochem. J. 327 (Pt 1) (1997) 105–115.
[19] M. Iwamori, S.E. Domino, Tissue-specific loss of fucosylated glycolipids in mice with targeted deletion of alpha(1, 2)fucosyltransferase genes, Biochem. J. 380 (2004) 75–81.
[20] B. Lin, M. Saito, Y. Sakakibara, et al., Characterization of three members of murine alpha1,2-fucosyltransferases: change in the expression of the Se gene in the intestine of mice after administration of microbes, Arch. Biochem. Biophys. 388 (2001) 207–215.
[21] S.E. Domino, L. Zhang, P.J. Gillespie, et al., Deficiency of reproductive tract alpha(1,2)fucosylated glycans and normal fertility in mice with targeted deletions of the FUT1 or FUT2 alpha(1,2)fucosyltransferase locus, Mol. Cell. Biol. 21 (2001) 8336–8345.
[22] T. Nochi, Y. Yuki, A. Matsumura, et al., A novel M cell-specific carbohydrate-targeted mucosal vaccine effectively induces antigen-specific immune responses, J. Exp. Med. 204 (2007) 2789–2796.
[23] I. Okayasu, S. Hatakeyama, M. Yamada, et al., A novel method in the induction of reliable experimental acute and chronic ulcerative colitis in mice, Gastroenterology 98 (1990) 694–702.
[24] T. Kunikata, H. Araki, M. Takeeda, et al., Prostaglandin E prevents indomethacin-induced gastric and intestinal damage through different EP receptor subtypes, J. Physiol. Paris 95 (2001) 157–163.
[25] K. Hase, K. Kawano, T. Nochi, et al., Uptake through glycoprotein 2 of FimH(+) bacteria by M cells initiates mucosal immune response, Nature 462 (2009) 226–230.
[26] A. Gebert, S. Fassbender, K. Werner, et al., The development of M cells in Peyer's patches is restricted to specialized dome-associated crypts, Am. J. Pathol. 154 (1999) 1573–1582.
[27] S. Onishi, T. Yokoyama, K. Chin, et al., Ultrastructural study on the differentiation and the fate of M cells in follicle-associated epithelium of rat Peyer's patch, J. Vet. Med. Sci. 69 (2007) 501–508.
[28] F. Sierro, E. Pringault, P.S. Assman, et al., Transient expression of M-cell phenotype by enterocyte-like cells of the follicle-associated epithelium of mouse Peyer's patches, Gastroenterology 119 (2000) 734–743.
[29] K.A. Knoop, N. Kumar, B.R. Butler, et al., RANKL is necessary and sufficient to initiate development of antigen-sampling M cells in the intestinal epithelium, J. Immunol. 183 (2009) 5738–5747.

Int J Clin Oncol
DOI 10.1007/s10147-011-0280-9

ORIGINAL ARTICLE

Subsequent risks for cervical precancer and cancer in women with low-grade squamous intraepithelial lesions unconfirmed by colposcopy-directed biopsy: results from a multicenter, prospective, cohort study

Koji Matsumoto · Yasuo Hirai · Reiko Furuta · Naoyoshi Takatsuka · Akinori Oki · Toshiharu Yasugi · Hiroo Maeda · Akira Mitsuhashi · Takuma Fujii · Kei Kawana · Tsuyoshi Iwasaka · Nobuo Yaegashi · Yoh Watanabe · Yutaka Nagai · Tomoyuki Kitagawa · Hiroyuki Yoshikawa · For Japan HPV and Cervical Cancer (JHACC) Study Group

Received: 29 March 2011 / Accepted: 15 June 2011

Abstract
Objective To investigate the natural course of low-grade squamous intraepithelial lesions (LSILs) that cannot be histologically confirmed by colposcopy-directed biopsy.
Methods In a multicenter, prospective, cohort study of Japanese women with LSILs, we analyzed the follow-up data from 64 women who had a negative biopsy result at the initial colposcopy (biopsy-negative LSIL) in comparison with those from 479 women who had a histologic diagnosis of cervical intraepithelial neoplasia grade 1 (LSIL/CIN1). Patients were monitored by cytology and colposcopy every 4 months for a mean follow-up period of 39.0 months, with cytologic regression defined as two consecutive negative smears and normal colposcopy.
Results In women with biopsy-negative LSILs, there were no cases of CIN3 or worse (CIN3+) diagnosed within 2 years; the difference in the 2-year risk of CIN3+ between the two groups was marginally significant (0 vs. 5.5%; $P = 0.07$). The cumulative probability of cytologic regression within 12 months was much higher in the biopsy-

K. Matsumoto (✉) · A. Oki · H. Yoshikawa
Department of Obstetrics and Gynecology,
Graduate School of Comprehensive Human Science,
University of Tsukuba, Tsukuba 305-8575, Japan
e-mail: matsumok@mui.biglobe.ne.jp

Y. Hirai
Departments of Gynecology and Cytopathology,
Cancer Institute Hospital, Japanese Foundation
of Cancer Research, Tokyo 135-8550, Japan

R. Furuta · T. Kitagawa
Department of Pathology, Cancer Institute, Japanese Foundation
of Cancer Research, Tokyo 135-8550, Japan

N. Takatsuka
Department of Epidemiology and Preventive Medicine, Gifu
University Graduate School of Medicine, Gifu 501-1194, Japan

T. Yasugi · K. Kawana
Department of Obstetrics and Gynecology,
University of Tokyo, Tokyo 113-8655, Japan

H. Maeda
Department of Transfusion Medicine and Cell Therapy,
Saitama Medical Center, Saitama Medical University,
Saitama 350-8550, Japan

A. Mitsuhashi
Department of Reproductive Medicine,
Graduate School of Medicine, Chiba University,
Chiba 260-8670, Japan

T. Fujii
Department of Obstetrics and Gynecology,
Keio University School of Medicine, Tokyo 160-8582, Japan

T. Iwasaka
Department of Obstetrics and Gynecology, Faculty of Medicine,
Saga University, Saga 849-8501, Japan

N. Yaegashi
Department of Obstetrics and Gynecology, Tohoku University
School of Medicine, Sendai 980-8574, Japan

Y. Watanabe
Department of Obstetrics and Gynecology, Kinki University
School of Medicine, Osaka 589-8511, Japan

Y. Nagai
Department of Obstetrics and Gynecology, Faculty of Medicine,
University of the Ryukyus, Okinawa 903-0215, Japan

Published online: 13 July 2011

negative LSIL group (71.2 vs. 48.6%; $P = 0.0001$). The percentage of women positive for high-risk human papillomaviruses (hrHPVs) was significantly lower in the biopsy-negative LSIL group than in the LSIL/CIN1 group (62.1 vs. 78.4%; $P = 0.01$); however, the 12-month regression rate of biopsy-negative LSIL was similar between hrHPV-positive and -negative women (67.3 vs. 74.4%, $P = 0.73$).
Conclusion In women with biopsy-negative LSILs, the risk of CIN3+ diagnosed within 2 years was low; furthermore, approximately 70% underwent cytologic regression within 12 months, regardless of HPV testing results. Biopsy-negative LSILs may represent regressing lesions rather than lesions missed by colposcopy.

Keywords Low-grade squamous intraepithelial lesion · Colposcopy · Human papillomavirus · Cervical intraepithelial neoplasia

Introduction

In the Bethesda System for cytologic reporting, a low-grade squamous intraepithelial lesion (LSIL) represents mild cervical abnormalities, including cellular changes associated with human papillomavirus (HPV) infection and cervical intraepithelial lesion grade 1 (CIN1) [1]. However, approximately 15–20% of women with a cytologic interpretation of LSIL have a grade 2 (CIN2) or grade 3 (CIN3) cervical intraepithelial lesion, which are immediately treated with cervical ablation, loop electrosurgical excision procedure (LEEP) or cone biopsy [2, 3]. Therefore, women with LSILs usually undergo a colposcopy-directed biopsy for histologic evaluation of cervical abnormalities. Of the women with LSIL cytology, 40–60% are found to have a histologic diagnosis of CIN1 at the initial colposcopy, while 15–30% have a negative biopsy result [2, 3]. According to the 2006 American Society for Colposcopy and Cervical Pathology consensus management guidelines [4], the follow-up strategy for women with a negative biopsy result is identical to that of women with CIN1; that is, both groups are followed with either repeated cytology at 6 and 12 months or HPV testing at 12 months. However, the natural course of LSILs that cannot be histologically diagnosed by colposcopy-directed biopsy has not been well documented.

The Japan HPV and Cervical Cancer (JHACC) cohort study was designed to identify determinants of regression and progression of low-grade cervical abnormalities [5, 6]. In the primary analysis, we used only the follow-up data from 570 women with cytologic LSIL and histologically confirmed CIN1 or CIN2 lesions, and demonstrated HPV type-specific risks of LSIL persistence and progression [5]. In the present study, we analyzed the follow-up data of 64 women with biopsy-negative LSIL who were excluded from the main analysis cohort.

Methods

Study design

This study represents a secondary analysis of data from the prospective non-intervention cohort study conducted by the JHACC study group for identifying determinants of LSIL/CIN regression and progression. Details of the design, methods, and primary results have been provided in more detail elsewhere [5, 6]. Briefly, 905 women with mildly abnormal cytology were recruited from nine hospitals that performed conventional Pap smears, colposcopy and cervical biopsies. The inclusion criteria of this secondary analysis were: evident LSIL cytology; histologic diagnosis of CIN1 or less at initial colposcopy and biopsy; age 18–54 years; first detection of cervical abnormality; and a sufficient number (two or more) of follow-up visits. Women entered the study voluntarily after giving their signed informed consent. Cervical smears were classified according to the Bethesda System [1]. At the time of study entry, two (or more) small cervical specimens were taken by colposcopy-directed punch biopsy and stained with hematoxylin and eosin (H&E). A histologic diagnosis was determined based on the World Health Organization (WHO) classification system. Two cytopathologists (Y.H. and Masafumi Tsuzuku) and two pathologists (R.F. and T.K.) reviewed all cytologic and histologic specimens collected at the time of entry. Patients were tested for cervical HPV DNA, serum IgG antibodies to cytomegalovirus (CMV), *Chlamydia trachomatis*, and herpes simplex virus type 2 (HSV2) at the time of entry. The researchers who performed the assays were blinded to the clinical data collected from the study subjects. Information regarding smoking and sexual behavior was obtained from a self-administered questionnaire. Patients were routinely followed at 3- to 4-month intervals and received cytologic and colposcopic examinations at each visit. To avoid interference from the biopsy procedure on the natural course of the disease, a cervical biopsy was performed during the follow-up period only when Pap smears and colposcopic findings were suggestive of the presence of CIN3 or worse (CIN3+). A cytology result of HSIL triggered colposcopy-guided biopsy during follow-up examinations. The two cytopathologists and the two pathologists reviewed all cytologic and histologic specimens collected for the diagnosis of CIN3+. We chose an end-point of CIN3 or cancer rather than CIN2 or higher because CIN2 likely represents a heterogenous collection of cervical abnormalities [7, 8], only some of which progress to CIN3 [5, 9]. In this analysis, we defined regression as normal colposcopy results and at least two consecutive negative Pap smears. Persistent lesions were defined as lesions that did not regress or were diagnosed with CIN3+ during the follow-up period.

Overall, the study subjects consisted of 554 women who had a negative biopsy result (biopsy-negative LSIL; $n = 64$) or a histologic diagnosis of CIN1 (LSIL/CIN1; $n = 491$) at the initial colposcopy for LSIL cytology. Unfortunately, data from cervical samples, blood samples, or questionnaires were not available in all 554 study subjects. Cervical HPV data were not available in 21 women because of insufficient samples, while data on serum antibodies to sexually transmitted agents were lacking in 23 women. In addition, 54 women gave no responses to a self-administrated questionnaire. The study protocol was approved by the ethical and research review boards of the participating institutions.

HPV genotyping

We detected HPV DNA in cervical samples by polymerase chain reaction (PCR)-based methodology, as previously described [10]. In brief, exfoliated cells from the ectocervix and endocervix were collected in a tube containing 1 ml of phosphate-buffered saline (PBS) and stored at −30°C until DNA extraction. Total cellular DNA was extracted from cervical samples by a standard sodium dodecyl sulfate (SDS)–proteinase K procedure. HPV DNA was PCR amplified by using consensus primers (L1C1/L1C2 + L1C2M) for the HPV L1 region. A reaction mixture without template DNA was included in every set of PCR runs as a negative control. Primers for a fragment of the β-actin gene were also used as a control to rule out false-negative results for samples in which HPV DNA was not detected. HPV types were identified by an analysis of restriction fragment length polymorphism (RFLP), which has been shown to identify at least 26 types of genital HPVs [11].

IgG antibody against sexually transmitted agents

The level of IgG antibodies to *Chlamydia trachomatis* and HSV2 was determined by using commercially available enzyme-linked immunosorbent assay (ELISA) kits: *Chlamydia trachomatis* (HITAZYME; Hitachi Chemical, Tokyo, Japan) and HSV2 (HerpeSelect 2 ELISA IgG; Focus Diagnostics, Cypress, CA, USA). The serologic assay for *Chlamydia trachomatis* utilizes purified EB outer-membrane proteins of the *Chlamydia trachomatis* L2 strain as antigens and does not detect antibody to *Chlamydia pneumoniae* [12]. These serologic assays were performed at a clinical testing laboratory (SRL, Tokyo, Japan).

Statistical analysis

All time-to-event analyses were based on the actual date of the visits. For regression or progression, time to event was measured from the date of the index visit (i.e., the first instance of an abnormal cytology result) to the date of the visit at which cytologic transition to normal occurred or CIN3+ was first detected. Women whose lesions persisted or who dropped out of the study were censored at their last recorded return visit dates. Subjects who had only one negative colposcopy/cytology result before loss to follow-up were censored at the last date of positive Pap tests. Subjects who were biopsied were censored at the time of their biopsy, regardless of the biopsy results, to reduce the potential for interference by the biopsy procedure on estimates of time of regression. Cumulative probability of LSIL regression or progression was estimated by using the Kaplan–Meier method and compared with a log-rank test. All analyses were carried out using the JMP 7.0J (SAS Institute, Cary, NC, USA) statistics packages. Two-sided P values were calculated throughout and considered to be significant at less than 0.05.

Results

We analyzed the follow-up data from a total of 554 women with LSIL cytology who had a negative biopsy result (biopsy-negative LSIL; $n = 64$) or a histologic diagnosis of CIN1 (LSIL/CIN1; $n = 491$) at the initial colposcopy. Distributions of baseline characteristics between these two groups are presented in Table 1. The women with biopsy-negative LSILs were older than the women with LSIL/CIN1 (mean age ± SD 38.8 ± 9.2 vs. 36.2 ± 7.7 years); however, the difference in the age distribution between the two groups was only marginally significant ($P = 0.07$). Cervical HPV infections were found in 75.0% of women with biopsy-negative LSILs and in 84.6% of women with LSIL/CIN1 results and the difference was statistically significant ($P = 0.02$). The percentage of women positive for high-risk human papillomaviruses (hrHPVs) was also significantly lower in the biopsy-negative LSIL group than in the LSIL/CIN1 group (62.1 vs. 78.4%; $P = 0.01$). The percentage of women who had smoked was lower in the biopsy-negative LSIL group (32.6 vs. 48.7%), but the difference was only marginally significant ($P = 0.07$). The number of lifetime sexual partners was significantly greater among women with LSIL/CIN1 than among women with biopsy-negative LSILs ($P = 0.001$). The age at first sexual intercourse was also lower among women with LSIL/CIN1 compared to women with biopsy-negative LSILs, although the difference was only marginally significant ($P = 0.06$). Women with LSIL/CIN1 were likely to have a higher IgG antibody titer against *Chlamydia trachomatis* than women with biopsy-negative LSILs; however, the difference was not significant ($P = 0.25$). The IgG reactivity to HSV2 was similar between the two groups ($P = 0.82$). At least two

Table 1 Characteristics of the study subjects

	Cytology and histology		P values[†]
	Biopsy-negative LSIL ($n = 64$)[a]	LSIL/CIN1 ($n = 479$)	
Age (years)			
Mean (SD)	38.8 (9.2)	36.2 (7.7)	
18–29	11 (17.2%)	95 (19.8%)	0.07
30–39	21 (32.8%)	215 (44.9%)	
40+	32 (50.0%)	169 (35.3%)	
HPV typing			
Positive for high-risk types[b]	36 (62.1%)	359 (78.0)	0.01
Negative for high-risk types	22 (37.9%)	101 (22.0%)	
Positive for any HPV	48 (77.4%)	405 (88.0%)	0.02
Negative for any HPV	14 (22.6%)	55 (12.0%)	
Smoking			
Never smokers	37 (63.8%)	222 (51.3%)	0.07
Smokers	21 (36.2%)	211 (48.7%)	
Current smokers	16 (27.6%)	143 (33.0%)	
Former smokers	5 (8.6%)	68 (15.7%)	
Number of lifetime sexual partners			
1	23 (39.6%)	79 (18.1%)	0.001
2–3	13 (22.4%)	129 (29.5%)	
4+	22 (37.9%)	229 (52.4%)	
Age at first sexual intercourse (years)			
≤20	12 (20.3%)	147 (34.2%)	0.06
21–23	26 (44.1%)	179 (41.6%)	
≥24	21 (35.6%)	104 (24.2%)	
IgG antibodies to *Chlamydia trachomatis*			
Low	27 (45.0%)	166 (36.1%)	0.25
Mid	20 (33.3%)	150 (32.6%)	
High	13 (21.7%)	144 (31.3%)	
IgG antibodies to HSV2			
Low	23 (38.3%)	158 (34.3%)	0.82
Mid	19 (31.6%)	150 (32.6%)	
High	18 (30.0%)	152 (33.0%)	

[†] These P value were calculated by the χ^2 test

[a] Biopsy-negative LSIL denotes women with LSILs that had a negative biopsy result at the initial colposcopy

[b] HPV16, 18, 31, 33, 35, 39, 45, 51, 52, 56, 58, 59 and 68 were classified into high-risk HPV types

biopsies were taken at the initial colposcopy and there was no difference in the number of biopsies between the two groups.

Patients were monitored by cytologic and colposcopic testing at intervals of 3–4 months. Among women with biopsy-negative LSILs, no case was diagnosed with CIN3+ within 2 years; the difference in the cumulative risk of CIN3+ diagnosed within the next 2 years between the two groups was marginally significant (0 vs. 5.5%; $P = 0.07$ by log-rank test; Fig. 1a). In women with biopsy-negative LSILs, the majority of cytologic regression occurred within 12 months. The cumulative probability of cytologic regressions within 12 months was much higher in women with biopsy-negative LSILs than in women with LSIL/CIN1 (71.2 vs. 48.6%; $P = 0.0001$; Fig. 1b). The 2-year rate of cytologic regression was also significantly different between the two groups (75.1 vs. 64.0%; $P = 0.003$). Cytologic regression occurred more quickly in women with biopsy-negative LSILs than in women with LSIL/CIN1 (median time to regression: 6.3 vs. 12.4 months). In the women with biopsy-negative LSILs, the 12-month cumulative probability of cytologic regression was similar between hrHPV-positive and -negative women (67.3 vs. 74.4%; $P = 0.74$); median time to regression was also similar between hrHPV-positive and -negative women (5.4 vs. 7.7 months; $P = 0.45$; Fig. 2a). In women with LSIL/CIN1, however, detection of hrHPVs significantly influenced the 12-month rate of cytologic regression (hrHPV-positive [45.2%] vs. hrHPV-negative [62.6%]; $P = 0.006$; Fig. 2b).

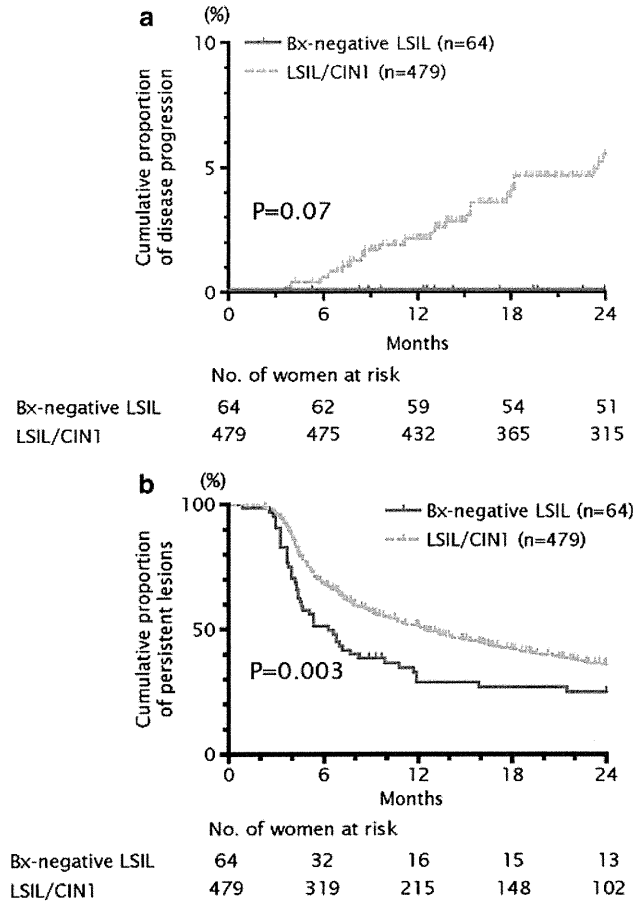

Fig. 1 Cumulative probabilities of CIN3+ diagnosis and cytologic regression within 2 years. A Kaplan–Meier plot was used to estimate the cumulative probabilities of CIN3+ diagnosis (**a**) and cytologic regression (**b**) within 2 years among women with biopsy-negative LSILs (*solid line*) or LSIL/CIN1 (*dashed line*). *P* values were calculated by the log-rank test

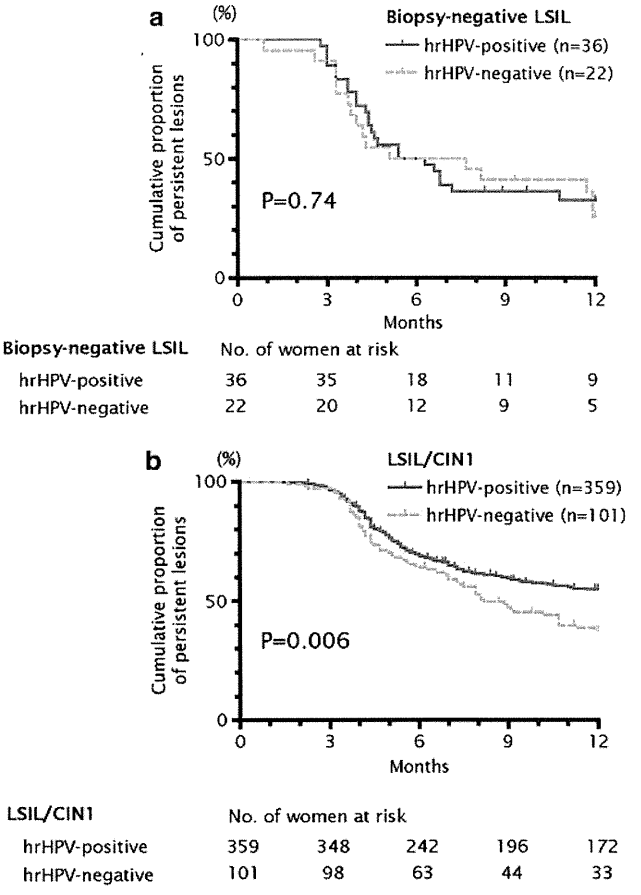

Fig. 2 Cumulative probabilities of cytologic regression within 12 months according to detection of hrHPVs. A Kaplan–Meier plot was used to estimate the cumulative probabilities of cytologic regression within 12 months among women with biopsy-negative LSILs (**a**) or LSIL/CIN1 (**b**) according to hrHPV detection. *P* values were calculated by the log-rank test

Discussion

Colposcopy-directed biopsies are recommended for women with LSIL cytology, primarily to exclude a high-grade lesion. Although approximately 15–30% of those women have a negative biopsy result [2, 3], they are routinely subjected to follow-up because of uncertainty about the risk of precancerous lesions missed by a colposcopic biopsy. In the present study, women with a biopsy-negative LSIL (i.e., "unconfirmed" LSIL) were at substantially low risk of CIN3 or cancer diagnosed within the following 2 years. The women with biopsy-negative LSILs were also significantly more likely to have cytologic regression than women with LSILs underlying CIN1. Some cases of biopsy-negative LSIL may be based on false-positive cytology because the percentage of women negative for any HPV was significantly higher in the biopsy-negative LSIL group than in the LSIL/CIN1 group. Additionally or alternatively, biopsy-negative LSILs may represent currently regressing lesions. This may be supported partially by the higher percentages of women in the biopsy-negative LSIL group who did not have cervical cancer risk factors, such as detection of hrHPVs, smoking, higher sexual activity and infections with *Chlamydia trachomatis* [13–16]. Several studies have reported that LSIL is more likely to regress to normal cytology among hrHPV-negative women or women who never smoked [5, 6, 17]. Interestingly, the 12-month regression rate of biopsy-negative LSIL was high, even among hrHPV-positive women. Low-grade lesions currently regressing to normal cytology may be difficult to confirm by colposcopy-guided biopsies because of the small lesion size, lower-grade colposcopic impression and/or weak pathologic findings.

Data on the natural course of biopsy-negative LSILs are limited. Pretorius et al. [18] reported that the subsequent risk of CIN3+ among women with histologically unconfirmed atypical squamous cells of undetermined significance (ASC-US) or LSIL cytology was low (1.8%). This

result was consistent with our observation; however, it was based on retrospective analyses of previous data including ASC-US cytology. In the ALTS (ASCUS-LSIL Triage Study) report [2], the risk of CIN3+ diagnosed within 2 years after unconfirmed LSIL was higher compared with the present study (6.1 vs. 0%). The difference between our results and the ALTS data may be explained by the difference in study design between the two studies. In the ALTS study, all women had an exit colposcopy and biopsy at 2 years after the semiannual follow-up by repeated cytology. Although our study subjects received both cytologic and colposcopic examinations at each visit at 3- to 4-month intervals, we did not routinely perform a colposcopic biopsy 2 years later. This may have resulted in an underestimation of the 2-year risk for CIN3+ in our study. Additionally, the sensitivity of the enrollment colposcopy may have affected the results from these two prospective studies. Recent studies have showed that initial colposcopy-directed biopsy are not as sensitive as we had previously assumed [19]. Thus, at least two directed biopsies, random biopsy or endocervical curettage are recommend to increase the sensitivity of the initial colposcopy [20–22]. In the ALTS study, 77.6% of women had null or only one biopsy at enrollment colposcopy [20]. By contrast, two (or more) biopsies were taken at entry in our study subjects. The number of biopsies may have increased the risk of misclassification errors of cervical lesions at enrollment. Although central pathologic review systems were employed in both studies, the limitation of histopathologic diagnosis (i.e., poor reproducibility in CIN grading) may also have affected disease classification at enrollment and during follow-up [7, 8, 23].

The current US guidelines advise that women with LSIL cytology and a histologic diagnosis of CIN1 or less should be followed with repeated cytology at 6 and 12 months or, alternatively, hrHPV testing at 12 months [4]. Our data also confirmed that these management strategies are sufficiently safe. A previous study reported that there was no significant difference in the subsequent risk of CIN2/3 between women with no disease documented by initial colposcopy-directed biopsy and women with histologically confirmed CIN1 [24]. However, the study was based on retrospective analyses, which was limited by the small sample size (negative biopsy $n = 43$; CIN1 $n = 30$) and included women with various cytologic abnormality profiles. In the present study, the risk of CIN3+ diagnosed within the following 2 years and the likelihood of LSIL regression were obviously different between women with biopsy-negative LSILs and women with LSIL/CIN1. The 2-year follow-up in ALTS of women with CIN1 or less has indicated that the subsequent risk of CIN2 or higher varies little with respect to the findings at the initial colposcopy [2]. However, when the analysis was confined to the risk of CIN3 or higher among women with LSILs, there was a marginal tendency for a higher risk of subsequent CIN3 that was associated with CIN1 compared with <CIN1 (10.5 vs. 6.1%). Based on these observations, the follow-up strategy for women with biopsy-negative LSILs may be better differentiated from that for women with LSIL/CIN1 results in terms of quality-of-life and cost. Our data suggest that follow-up by repeated cytology at 12 months may be appropriate for women with biopsy-negative LSIL when two or more colposcopy-directed biopsies are taken at the initial colposcopy.

In conclusion, the risk of CIN3+ diagnosed within 2 years was low in women with biopsy-negative LSILs; furthermore, approximately 70% showed cytologic regression within 12 months, regardless of HPV testing results. Our data suggest that biopsy-negative LSILs may represent false-positive cytology or currently regressing lesions rather than lesions missed by colposcopy. However, the sample size of the present study was small; thus, to confirm our results, further prospective studies with larger sample sizes will be needed.

Acknowledgments The authors thank Dr. Tadahito Kanda (Center for Pathogen Genomics, National Institute of Infectious Diseases, Tokyo, Japan) for his comments on the study design and the manuscript; Mr. Masafumi Tsuzuku (Department of Cytopathology, Cancer Institute Hospital, Japanese Foundation of Cancer Research, Japan) for his cytologic review; many other researchers who facilitated this study; and all the women who participated in the study. This work was supported by a grant from the Ministry of Education, Science, Sports and Culture of Japan (grant # 12218102).

Conflict of interest We declare that we have no conflict of interest relevant to this article. The supporting organization played no role in the design and implementation of the study; the collection, management, analysis, and interpretation of the data; and the preparation, review, or approval of the manuscript.

References

1. Solomon D, Davey D, Kurman R et al (2002) The 2001 Bethesda system: terminology for reporting results of cervical cytology. JAMA 287:2114–2119
2. Cox JT, Schiffman M, Solomon D et al (2003) Prospective follow-up suggests similar risk of subsequent cervical intraepithelial neoplasia grade 2 or 3 among women with cervical intraepithelial neoplasia grade 1 or negative colposcopy and directed biopsy. Am J Obstet Gynecol 188:1406–1412
3. Wentzensen N, Schiffman M, Dunn ST et al (2009) Grading the severity of cervical neoplasia based on combined histopathology, cytopathology, and HPV genotype distribution among 1,700 women referred to colposcopy in Oklahoma. Int J Cancer 124:964–969
4. Wright TC Jr, Massad LS, Dunton CJ et al (2007) 2006 consensus guidelines for the management of women with abnormal cervical cancer screening tests. Am J Obstet Gynecol 197:346–355
5. Matsumoto K, Oki A, Furuta R et al (2011) Predicting the progression of cervical precursor lesions by human papillomavirus